



1 **Modeling of greenhouse gas emissions from paludiculture in**
2 **rewetting peatlands is improved by high frequency water table**
3 **data**

4 **Andres F. Rodriguez¹, Johannes W.M. Pullens^{1,2}, Jesper R. Christiansen³, Klaus S.**
5 **Larsen³, and Poul E. Lærke^{1,2}**

6 ¹ Department of Agroecology, Aarhus University, Tjele, 8830, Denmark

7 ² iCLIMATE Interdisciplinary Centre for Climate Change, Aarhus University, Roskilde,
8 4000, Denmark

9 ³ Department of Geosciences and Natural Resource Management, University of Copenhagen,
10 Copenhagen, 1958, Denmark

11

12 *Correspondence to:* Andres F. Rodriguez (afrodriguez@agro.au.dk)

13 **Abstract**

14 Rewetting drained peatlands can reduce CO₂ emissions but prevents traditional agriculture.
15 Crop production under rewetted conditions may continue with flood-tolerant crops in
16 paludiculture, but its effects on greenhouse gas (GHG) emissions compared to rewetting
17 without further management are largely unknown. This study was conducted between 2021
18 and 2022 on a fen peatland in central Denmark. At the study site, three harvest/fertilization
19 management treatments were implemented on Reed Canary Grass (RCG) established in 2018.
20 Measurements of CO₂ and CH₄ emissions were conducted biweekly using a transparent
21 manual chamber connected to a gas analyzer and manipulating light intensities with four
22 shrouding levels. Although this was a rather wet peatland (-8 cm mean annual WTD), the site



23 was a CO₂ source with a mean net ecosystem C balance (NECB) of 6.5 t C ha⁻¹ yr⁻¹ across
24 treatments. Model simulation with the use of high temporal resolution water table depth
25 (WTD) data was able to better capture ecosystem respiration (R_{eco}) peaks compared to the use
26 of mean annual WTD, which underestimated R_{eco}. Data on pore water chemistry further
27 improved statistical linear models of CO₂ fluxes using soil temperature (Ts), WTD, ratio
28 vegetation indices and PAR as explanatory variables. Significant differences in CO₂
29 emissions and water chemistry parameters were found between studied blocks, with higher
30 R_{eco} corresponding to blocks with higher pore water nutrient concentrations. Methane
31 emissions averaged 113 kg of CH₄ ha⁻¹ yr⁻¹, equivalent to 11.3% of the total carbon emission
32 in CO₂ equivalents. Because of large heterogeneity among the experimental blocks no
33 significant treatment effect was found, however, the results indicate that biomass harvest
34 reduces GHG emission from productive rewetted peatland areas in comparison with no
35 management, whereas on less productive areas it is beneficial to leave the biomass
36 unmanaged.

37 **1 Introduction**

38 Peatlands are an essential component of the global C cycle. Covering only 3% of the
39 terrestrial surface they store ~600 Gt of C, equivalent to 30% of the global soil C pool and
40 exceeding the C stored in vegetation by ~150 Gt (Yu et al., 2010; Scharlemann et al., 2014;
41 Erb et al., 2018; Leifeld and Menichetti, 2018). Northern temperate peatlands can be
42 classified as bogs or fens and store 21.9 Gt C (Leifeld and Menichetti, 2018). While bogs are
43 rain fed and nutrient poor, fens receive drain and ground water from the upland and
44 occasionally from the streams under flooding conditions making them minerotrophic with a
45 pH close to neutral because the incoming waters carry minerals released from surrounding
46 soils and sediments. Under high nutrient concentrations, fens are dominated by grasses and
47 sedges such as *Phragmites sp.* and *Cladium sp.* (Page and Baird, 2016; Kreyling et al., 2021).



48 Peatland drainage creates aerobic conditions leading to peat mineralization, and consequently
49 soil C is emitted as CO₂ to the atmosphere (Page and Baird, 2016), and dissolved C and N
50 compounds are leached from the soil (Cabezas et al., 2012; Liu et al., 2019). Emissions from
51 drained peatlands are estimated globally to 785 Mt CO₂ equivalents and the water table is
52 considered the main controlling factor (Zhong et al., 2020; Evans et al., 2021) with higher
53 water tables resulting in lower CO₂ emissions (Tiemeyer et al., 2020; Evans et al., 2021;
54 Koch et al., 2023). However, other factors such as soil temperature (Ts), vegetation, and
55 nutrient status may also affect CO₂ emissions from drained peat soils (Wilson et al., 2016;
56 Rigney et al., 2018; Bockermann et al., 2024). When peatlands are drained, the peat bulk
57 density increases (Liu et al., 2019; Loisel and Gallego-Sala, 2022), and peat chemistry
58 changes leading to decreasing C:N ratio, increased concentrations of humic compounds,
59 polyphenols, dissolved organic C (DOC) and N (DON), and NH₄. The changes in peat
60 chemistry may in turn enhance organic matter mineralization (Cabezas et al., 2012; Liu et al.,
61 2019; Zak et al., 2019), and the release of nutrients along with higher bacterial and fungal
62 activity increases CO₂ emissions (AminiTabrizi et al., 2022; Song et al., 2022).

63 The importance of peatlands for C storage and GHG emission mitigation, as well as other
64 environmental services, has sparked an interest in peatland restoration with focus on
65 rewetting (Page and Baird, 2016; Andersen et al., 2017). While rewetting reduces CO₂
66 emissions, it also may lead to increased CH₄ emissions (Wilson et al., 2016; Zhong et al.,
67 2020; Darusman et al., 2023). The CO₂ / CH₄ emission trade-off depends on the water table,
68 the origin of the water (bog/fen), type of vegetation (Rigney et al., 2018; Purre et al., 2019),
69 its nutrient status (Wilson et al., 2016; Tiemeyer et al., 2020), as well as gradual changes in
70 the microbial community following rewetting (Putkinen et al., 2018; Hemes et al., 2019;
71 Emsens et al., 2020; Urbanova and Barta, 2020).



72 Rewetting can be achieved through different pathways depending on the land use in the
73 peatland after raising the water table. Often, peatlands are rewetted either without altering the
74 established plant community or by attempting to reestablish the plant communities present in
75 pristine peatlands. Paludiculture has been suggested as an alternative land use of rewetted
76 peatlands enabling continued agricultural biomass production under low or high management
77 intensity (Tanneberger et al., 2020; Ziegler, 2020). It can also reduce CO₂ emissions due to
78 the water-saturated conditions of the peat soils (Ren et al., 2019; Tanneberger et al., 2020; De
79 Jong et al., 2021) while producing biomass for renewable energy such as biogas production
80 (Dragoni et al., 2017; Ren et al., 2019; Hartung et al., 2020) or material that can be used as a
81 green alternative in the building industry. Paludiculture may also have the potential to remove
82 excess nutrients from rewetted peatlands (Giannini et al., 2017; Vroom et al., 2018; Geurts et
83 al., 2020). Large variation in quantified annual GHG emission from different land use of
84 rewetted peatlands have been reported and further studies are needed to establish emission
85 factors for them (Bianchi et al., 2021).

86 It is well known that greenhouse gas emissions from rewetted peatlands are influenced by
87 their nutrient content and water table level reflected by IPCC Tier 1 emissions factors
88 (Wilson et al., 2016). Mean annual water table depth has also been used to predict the net
89 ecosystem carbon balance (NECB), but much uncertainty remains unexplained (Tiemeyer et
90 al., 2020; Evans et al., 2021; Koch et al., 2023). The complexity and temporal resolution of
91 gap filling models can also influence the NECB estimates (Karki et al., 2019; Liu et al., 2022)
92 and it is highly uncertain how water table dynamics during the year, as well as nutrient status
93 and different management practices affect annual emission budgets. Consequently, the
94 objectives of this study were to: (1) determine the NECB of reed canary grass (RCG)
95 production under three harvest and fertilization management strategies during the third year
96 after establishment in a peatland with shallow WTD (2) assess model performance in gap

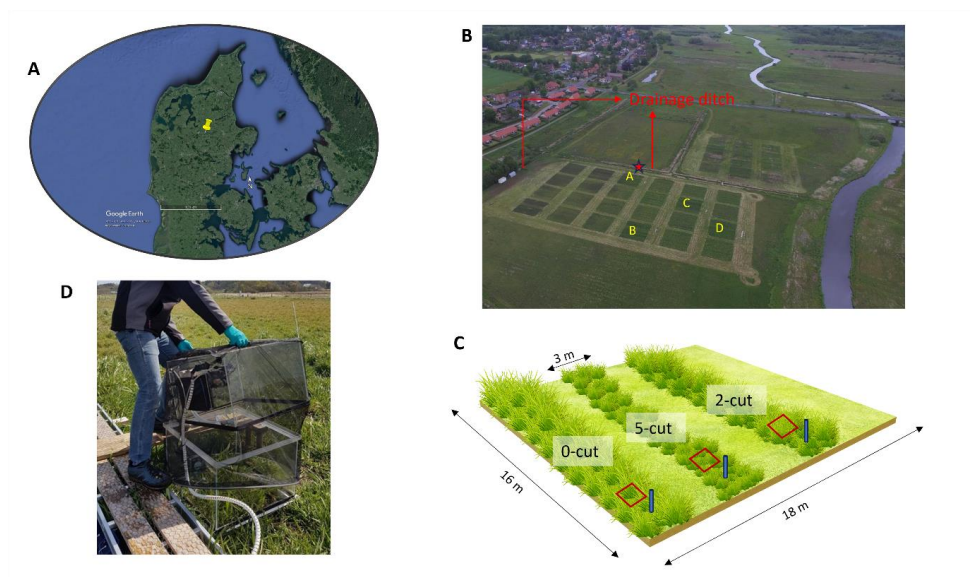


97 filling biweekly measurements of ecosystem respiration (R_{eco}) and gross primary productivity
98 (GPP) using high temporal resolution data on water table depth (WTD) and (3) investigate
99 the relation of soil water chemistry with R_{eco} and GPP. We hypothesized that fertilization and
100 harvesting RCG would increase C emissions compared to no RCG management, that the use
101 of high-temporal frequency data on water table depth (WTD) would improve model
102 prediction of ecosystem respiration (R_{eco}), and that the addition of soil pore water chemistry
103 parameters as explanatory variables would improve the explanation of C fluxes.

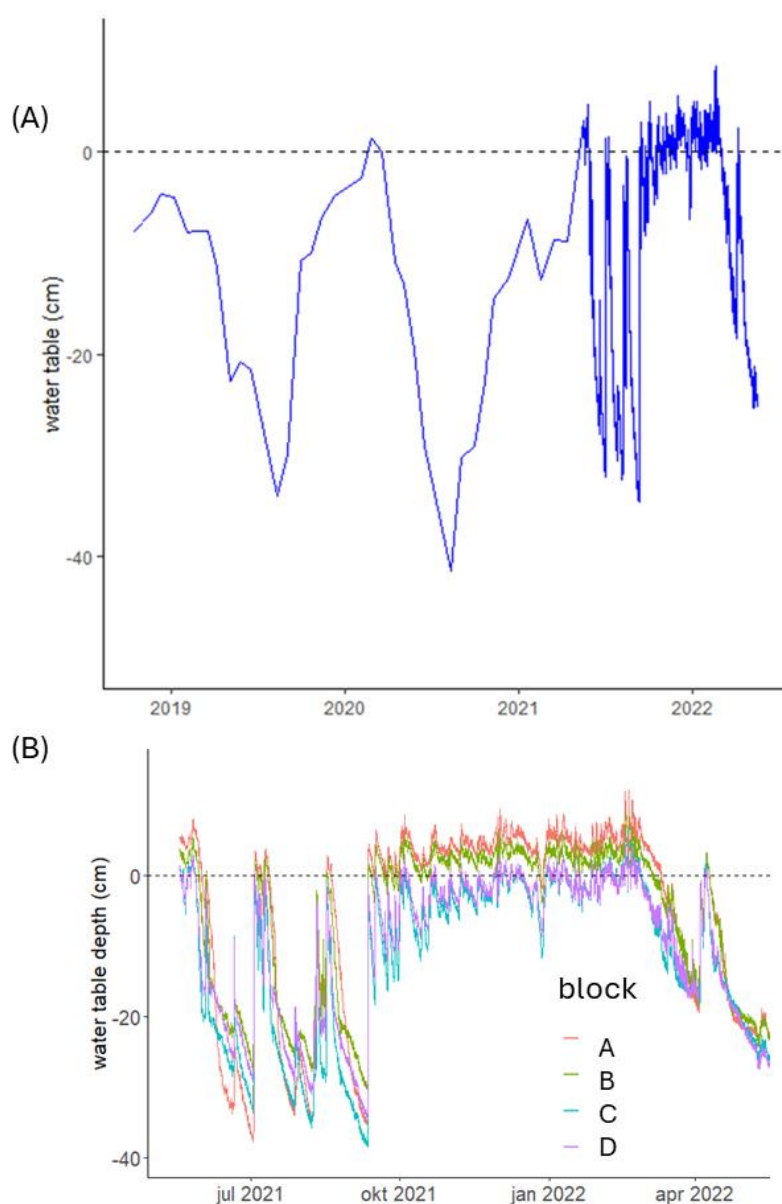
104 **2 Materials and methods**

105 **2.1 Study area**

106 This study was conducted from May 2021 to May 2022 at a riparian fen peatland located in
107 the Nørreå valley, Vejrumbro, Central Jutland, Denmark (56°26'15.3''N, 9°32'44.1''E) (Fig
108 1). The site was drained in the 1930s and used for agriculture predominantly under grassland
109 rotation and grazing. The field became gradually wetter because of land subsidence, and the
110 water level was largely controlled by the Nørreå stream, located at the southern border of the
111 peatland (Malinowski et al., 2015). After 2018, maintenance of the drainage ditches stopped
112 and the mean annual WTD across the experimental plots gradually increased during the
113 following years reaching -8 cm during the study year, with a mean minimum of -35 cm in the
114 summer and a mean maximum of 8 cm in the winter (Fig 2a). The mean air temperature and
115 total precipitation, measured at the Foulumgard meteorological station (Danish
116 Meteorological Institute), located 6 km from the study site, were 9 °C and 709 mm,
117 respectively. The peat layer at the study site has an average depth of 2 m covering up to 10 m
118 of gyttja (Mashadi et al., 2024). The physicochemical characteristics of the peat were
119 measured for the top 1 meter of the soil as part of a previous study (Table 1) by Nielsen et al.
120 (2023b).



121
 122 Figure 1. A, map of Denmark indicating the study site location © Google Earth; B, aerial
 123 photograph of study site, letters indicate the four studied blocks, and red star indicates where
 124 the ditch water samples were taken from; C, diagram of one of the blocks showing the three
 125 randomized harvest treatment plots (0-cut, 2-cut, and 5-cut) and the location of collars (red
 126 squares) and piezometers (blue cylinders); D, transparent chamber with shroud used for gas
 127 measurements.



128

129 Figure 2. (A) Water table depth at the study site from October 2018, from Oct 2018 to Apr
 130 2021 data was collected biweekly, from May 2021 until May 2022 data was collected hourly.
 131 (B) Hourly water table depth per plot during the studied year. Values are average of plots.
 132 Colors indicate different blocks.



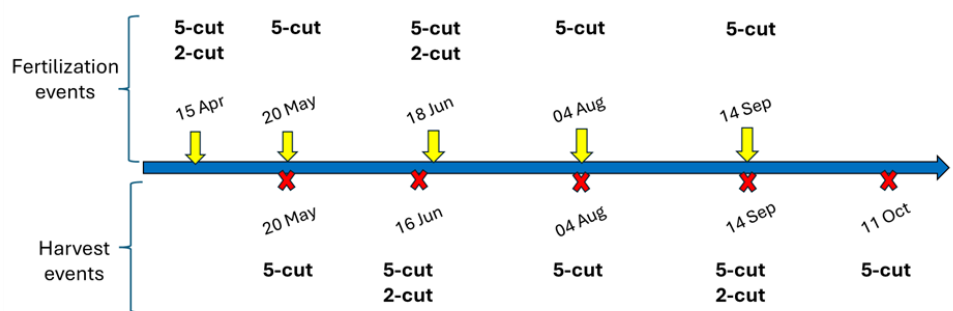
133 Table 1. Soil physicochemical characteristics at the study site of the four studied plots (A-D).
 134

Plot	OM	pH	pb	TC	TN	C:N
	%		g cm ⁻³	g kg ⁻¹	g kg ⁻¹	g kg ⁻¹
A	85	5.6	0.15	440	26	17
B	83	6.0	0.15	430	28	14
C	70	6.2	0.18	374	24	15
D	75	6.2	0.13	401	27	15
Mean	78	6.0	0.15	411	26	15

135 †OM, organic matter; pb, bulk density; TC, total C; TN, total N; C:N, carbon to nitrogen
 136 ratio.

137 138 2.2 Experimental design

139 Four blocks (indicated by A, B, C and D on Fig 1B) were established with reed canary grass
 140 (RCG, *Phalaris arundinacea*, cultivar Lipaula) in 2018 as part of a larger field experiment.
 141 Each block had six randomly placed plots with treatments of different combined effects of
 142 harvest and fertilization whereof only three (0-cut, 2-cut, 5-cut) were used for this study.
 143 Harvest and fertilization dates can be seen in Figure 3. The harvested plots were fertilized
 144 with 200 kg N ha⁻¹ and 178 kg K ha⁻¹ in total, given as NPK 18-0-16 in equal split doses.
 145 Thus, the 2-cut and the 5-cut received 100 kg N ha⁻¹ and 40 kg N ha⁻¹ for each cut,
 146 respectively, while the 0-cut did not receive any fertilizer. The dimensions of the blocks and
 147 plots were (16 x 18 m), and (16 x 3 m), respectively (Fig 1C). Further details of the
 148 experimental design can be found in Nielsen et al. (2021). At each plot, one 55 x 55 cm collar
 149 was installed to 10 cm depth to facilitate closed, none-steady-state chamber measurements of
 150 net CO₂ and CH₄ fluxes. A piezometer with a screen from 5 cm to 100 cm soil depth was
 151 installed 10-20 cm away from the collar for soil water sampling. Ts at 5 cm soil depth and
 152 WTD were continuously measured using Ts dataloggers (HOBO Pendant temperature/light
 153 64K data logger; Onset Corporation, Massachusetts, USA), and Leveloggers (Levellogger 5
 154 Junior; Solinst Canada Ltd, Ontario, Canada), respectively. Perforated gauge tubes for
 155 leveloggers sealed with lids and soil temperature loggers were installed in 2020 inside the
 156 collars.



157

158 Figure 3. Timeline of fertilization and harvest events applied to the 2-cut and 5-cut harvest
159 treatments during 2021 at the studied blocks.

160

161 **2.3 Net carbon dioxide and methane flux measurements**

162 The CO₂ and CH₄ measurements were performed biweekly +/- one week depending on
163 meteorological conditions between the 28th of May 2021 and the 14th of June 2022. A total of
164 26 campaign measurements were undertaken. Fluxes were measured using a fully transparent
165 chamber (60 cm x 60 cm x 41 cm) made of Plexiglass and equipped inside with a
166 photosynthetic active radiation (PAR) sensor (190-SA; Li-Cor Inc., Lincoln, NE, USA), a
167 temperature sensor, and an air mixing fan. Further details of the chamber design and how the
168 temperature was controlled during operation can be found in Elsgaard et al. (2012). The
169 chamber was connected to an LGR-ICOSTM GLA131-GGA microportable gas analyzer (ABB
170 Ltd.), which simultaneously measured water vapor corrected CO₂ and CH₄ (i.e., dry
171 fractions) at 1 Hz resolution. Chamber deployment was 120 sec per measurement. All data
172 were stored in a Campbell CR1000X data logger (Campbell Sci. Logan, UT, USA) with the
173 same timestamp. In order to fit the RCG inside the chamber during growth, a chamber
174 extension with the same dimensions as the measurement chamber was used during all
175 measuring campaigns, i.e. total chamber height with the extension was 82 cm. Measurements
176 were performed between 10:00 am and 3:00 pm on predominantly clear days without
177 precipitation. Measurements were conducted during constant PAR conditions, when possible,



178 by timing measurements such that changing cloud conditions were avoided. For each
 179 campaign and at each soil collar, fluxes were measured corresponding to four PAR levels by
 180 using net shrouds and an opaque cover as described by Kandel et al. (2017). This resulted in
 181 four flux measurements, one under fully transparent conditions which corresponded to net
 182 ecosystem exchange (NEE), a second under ca. 50% blocked PAR, a third under ca. 75%
 183 blocked PAR, and a fourth under 100% blocked PAR equivalent to R_{eco} . Between PAR levels
 184 plants were given one minute to adapt to the new PAR conditions while the chamber was
 185 lifted on one side, allowing air circulation and bringing CO_2 and CH_4 concentrations to
 186 atmospheric levels.

187 All fluxes were calculated using the Flux package 0.3-0.1 (Jurasinski et al., 2022) in R (R
 188 Core Team (2023), R version 4.3.0). Inspection of fluxes revealed that fluxes were mostly
 189 linear, and flux rates were therefore calculated based on linear regression. For low CO_2 fluxes
 190 ($<100 \text{ mg } CO_2 \text{ m}^{-2} \text{ h}^{-1}$), fluxes with an $R^2 < 0.6$ and a $nrmse > 0.1$ were removed, while for
 191 high CO_2 fluxes ($>100 \text{ mg } CO_2 \text{ m}^{-2} \text{ h}^{-1}$), fluxes with an $R^2 < 0.9$ and a $nrmse > 0.1$ were
 192 identified and the PAR and CO_2 flux were manually inspected. If sudden changes in the PAR
 193 occurred during the 2 min measurement period or if the flux curve indicated a possible
 194 leakage, flux data were discarded. These criteria resulted in 3% of the calculated CO_2 fluxes
 195 being removed. In the case of CH_4 , all calculated fluxes had R^2 values higher than 0.9,
 196 therefore no fluxes were removed based on non-linearity, if a possible leakage was identified
 197 fluxes were removed, resulting in 1.6% of the fluxes removed. For further calculations, only
 198 the CH_4 fluxes measured under 100% PAR blocked (opaque conditions) were used.

199 **2.4 Biomass measurements**

200 Spectral reflectance was measured in all collars biweekly at gas sampling days and before
 201 and after harvest events using a portable crop sensor (RapidSCAN CS-45; Holland Scientific



Inc., Lincoln, NE, USA), which was held 30 cm above the canopy and horizontally rotated 45° while performing measurements to cover all vegetation inside the collar. Approximately 30 scans were taken per collar and their mean values were used to calculate the ratio vegetation index (RVI) as the ratio of near-infrared to red light reflectance. The RVI has been used as a proxy for photosynthetically active biomass and it has been used in photosynthesis and ecosystem respiration models (Kandel et al., 2017; Karki et al., 2019). Hourly RVI values were obtained by linearly interpolating biweekly RVI measurements, hourly values were used in GPP and R_{eco} modelling. Fresh weight yield and dry matter content was determined by harvesting the biomass inside the collars at respective cuts. This biomass was analyzed for total N and C with a Vario Max CN (Elementar Analysensysteme GmbH, Hanau, Germany). Dry matter yields (Table A1) were multiplied by percentage C to obtain the yield in $C\ ha^{-1}\ yr^{-1}$ as part of the CO_2 -C budget. The sum of yields from individual cuts per treatment was considered as the annual yield.

2.5 Gap filling models and annual budgets

The measured NEE CO_2 fluxes were partitioned into GPP and R_{eco} . The GPP was calculated as $NEE - R_{eco}$ and it was calculated for all PAR levels. From an atmospheric perspective we always consider R_{eco} positive, and GPP negative while NEE can be either positive (ecosystem carbon source) or negative (ecosystem carbon sink). The net ecosystem carbon balance (NECB) was calculated as the sum of the NEE plus the harvested yields of the 2-cut and 5-cut treatments. For calculation of annual budgets, three models from previous studies (one for GPP and two for R_{eco} , see below), which used RVI, Ts, and WTD were selected as explanatory variables. Additionally, a fourth model was developed based on a modification of the two selected R_{eco} models. The GPP was modelled based on Karki et al. (2019) (model 1).

$$GPP = \frac{GPP_{max} * PAR}{k + PAR} * \left(\frac{RVI}{RVI + \alpha} \right) * FT \quad (\text{model 1})$$



Where GPP is in $\text{mg CO}_2 \text{ m}^{-2} \text{ h}^{-1}$, RVI is the ratio vegetation index, k is the PAR value at which GPP reaches 50%, α is a fitted parameter, and FT is a linear temperature dependent function set to 0 when temperature $< -2^\circ \text{C}$ and to 1 when temperature $> 10^\circ \text{C}$ (Kandel et al. 2017).

R_{eco} was modelled based on Karki et al. (2019) with RVI and T_s as input variables (model 2), based on Rigney et al. (2018) with WTD and T_s as input variables (model 3), and with our developed model, which included RVI , WTD and T_s as input variables (model 4).

$$Reco = t1 + (a * RVI) * e^{\left[b * \left(\frac{1}{T_{10}-T_0} - \frac{1}{T_s-T_0}\right)\right]} \quad (\text{model 2})$$

$$Reco = t1 * e^{\left[b * \left(\frac{1}{T_{10}-T_0} - \frac{1}{T_s-T_0}\right)\right]} + (WTD + c)^2 \quad (\text{model 3})$$

$$Reco = t1 + (a * RVI) + [(WTD - WTD_{\text{max}}) * c]^2 * e^{\left[b * \left(\frac{1}{T_{10}-T_0} - \frac{1}{T_s-T_0}\right)\right]} \quad (\text{model 4})$$

Where R_{eco} is in $\text{mg CO}_2 \text{ m}^{-2} \text{ h}^{-1}$, RVI is the ratio vegetation index, WTD is the water table depth (cm), WTD_{max} is the maximum WTD (cm), $t1$, a , b , and c are fitted parameters, $t1$ has a lower limit set at 1, while all other fitted parameters are without upper and lower limits. T_{10} is the reference temperature set to 10°C , T_0 is the zero-respiration temperature set to -46°C , and T_s is the soil temperature ($^\circ \text{C}$) at 5 cm depth.

Each R_{eco} model was fitted to data obtained biweekly using non-linear regression (non-least square) in R (R Core Team (2023), R version 4.3.0) for each plot independently. Annual CO_2 budgets were calculated using the parameterized models, hourly T_s , WTD , and RVI . Model performance was evaluated by comparing the measured GPP and R_{eco} with the modelled values using the following indices: Nash-Sutcliffe efficiency, which indicates how well the plot of observed versus simulated data fits the 1:1 line, with more accurate models having values closer to 1, corrected Akaike information criterion (AICc), normalized root mean square error, and R^2 using the hydroGOF package in R (Zambrano-Bigiarini, 2020). Based on these criteria, the best performing R_{eco} model was used to calculate the annual CO_2 budget. In addition, field models of R_{eco} (model 4) and GPP were parameterized by pooling data from all blocks and treatment plots. For CH_4 , measured fluxes were linearly interpolated to obtain the annual CH_4 budget.



254 We tested the sensitivity of the best performing R_{eco} model (model 4) to the frequency of
255 WTD data either using (a) hourly WTD, Ts, and RVI (b) annual mean WTD with hourly Ts
256 and RVI, and (c) annual mean WTD, annual mean Ts, and hourly RVI.

257 **2.6 Water chemistry**

258 Soil pore water was collected biweekly at the same time as the gas campaigns and analyzed
259 for total organic C (TOC), dissolved organic C (DOC), total nitrogen (TN), total dissolved
260 nitrogen (TDN), nitrate-N, (NO_3), ammonia-N (NH_4), total P (TP), total dissolved P (TDP),
261 Fe, pH, Electroconductivity (EC), and turbidity. Pore-water samples were collected
262 immediately after each GHG measurement from piezometers installed 20 cm from each GHG
263 collar. Water samples were extracted through a tube fitted at the end with an aquarium air
264 stone (Air Stone Economy Cylinder 4 X 5 cm, Aquakoi / JV Trading Aps) placed 20 cm
265 below the water table in each piezometer. An additional sample was collected from a ditch
266 draining the peatland. A total of 13 samples were collected per campaign for a total of 338
267 samples. Upon collection, part of the sample was filtered using 0.45 μm pore size filter. The
268 unfiltered samples were analyzed for pH and electroconductivity (EC) following the Danish
269 Standards DS287 and DS288, respectively, turbidity, TN following Best (1976), TP using the
270 Danish Standard, DS291 photometric method (Dansk Standard, 2004), TOC using a total
271 organic C analyzer (TOC-VCPH; Shimatzu Corporation, Kyoto, Japan), and Fe by ICP
272 emission spectrometer (iCAP 6000 series; Thermo Fisher Scientific, Inc., Waltham,
273 Massachusetts, USA). The filtered samples were analysed for DOC with a (TOC-VCPH;
274 Shimatzu Corpotation, Kyoto, Japan), TDN and NO_3 (Best, 1976), TDP by the Danish
275 Standard, DS291 photometric method (Dansk Standard, 2004), and NH_4 following Crooke
276 and Simpson (1971).

277 **2.7 Statistical analysis**



278 Statistics were performed in R (R Core Team (2023), R version 4.3.0). Effects were
 279 considered significant if $p\text{ value} < 0.05$. Normality assumptions were evaluated with Q-Q
 280 plots, histograms, and residual plots. Kruskal-Wallis tests were used to test the effect of
 281 harvest treatment and block on R_{eco} , GPP, NEE, and NECB. Correlations and principal
 282 component analysis (PCA) were used to establish relationships between water chemistry
 283 parameters, R_{eco} , GPP, NEE, Ts, RVI, PAR, WTD, and CH_4 .
 284 ANOVA and Tukey tests were used to determine differences between water chemistry
 285 parameters among blocks and harvest treatments. The effects of each water chemistry
 286 parameter on R_{eco} and GPP were tested with linear mixed models. Each water chemistry
 287 parameter was added one by one as a fixed factor to the base models shown below as models
 288 5 and 6, and the performance of the model including each water chemistry parameter was
 289 compared to the base model. The R_{eco} base model included WTD, Ts, and RVI as fixed
 290 factors and the measuring campaign and replicate block as random factor (model 5), while
 291 the GPP base model included PAR, Ts, and RVI as fixed factors and measuring campaign and
 292 replicate block as random factors (model 6).
 293 (model 5) $Reco = Harvest\ treatment + WTD + Ts + RVI + (campaign) + (R.Plot)$
 294 (model 6) $GPP = Harvest\ treatment + PAR + Ts + RVI + (campaign) + (R.Plot)$
 295 Likelihood ratio tests were used to establish if there was a significant improvement of the
 296 base models by adding the water chemistry parameters, if this was the case, the R^2 and root
 297 mean square error (RMSE) were calculated. Outliers of the water chemistry data were
 298 identified as being larger than 3 times the standard deviation for each parameter
 299 independently excluding 1% of the data from the analyses.

300 3. Results

301 3.1 Model performance



302 Measured R_{eco} was best described by model 4 in 11 out of the 12 studied plots based on the
 303 NSE and in 10 out of 12, based on the AICc (table 2). The other calculated indices (R^2 , and
 304 NRMSE) also supported model 4 as the best overall performing model. When WTD was
 305 excluded as seen in model 2 compared to model 4, the overall performance was reduced as
 306 indicated by lower NSE for most plots except for plot C 5-cut and plot D 0-cut (Table 2).
 307 Model 3, where RVI was excluded, had the lowest performance of the three tested models. In
 308 general, the 0-cut plots provided the best model performances with NSE and $R^2 > 0.9$ and the
 309 lowest AICc, while the 2-cut and 5-cut plots had lower model performances (between 0.74
 310 and 0.92 NSE). The performance results for the GPP models had R^2 values that ranged
 311 between 0.81 and 0.96 (Table A3). These results show that the GPP models had R^2 values that
 312 ranged between 0.81 and 0.96.

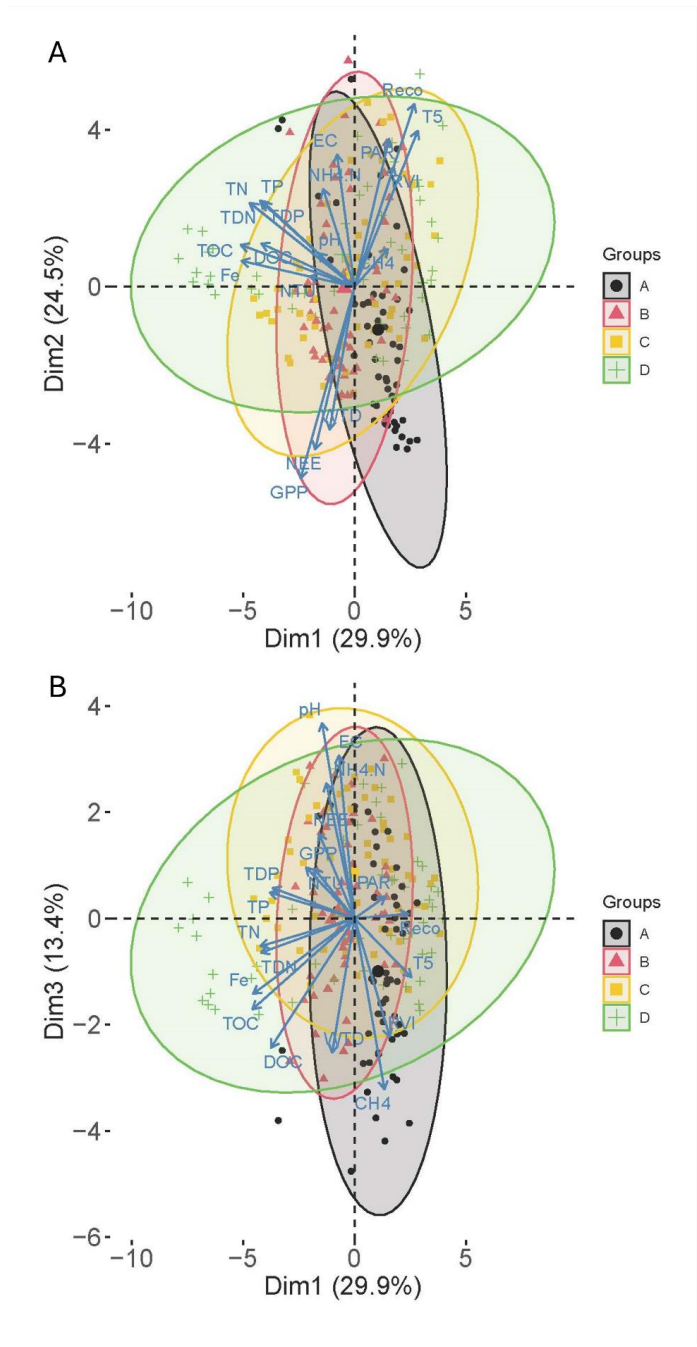
313 R_{eco} was positively correlated with Ts and RVI, and negatively correlated to WTD (lower
 314 WTD = deeper WTD). On the other hand, GPP was negatively correlated to Ts, RVI, and
 315 PAR. These expected relationships seen in PCA plots (Fig 4) and correlations (Fig. A1)
 316 support why the variables in models 1-4 were selected and parameterized in this study. The
 317 fitted parameter values of the best performing R_{eco} model and the GPP model varied between
 318 plots (Fig 5). For the R_{eco} model, the b parameter was near its maximum value in most plots,
 319 while for the GPP model, the k parameter was near its maximum in most plots.



Table 2. Evaluation of three R_{eco} models parameterized for each plot by four different performance indices.

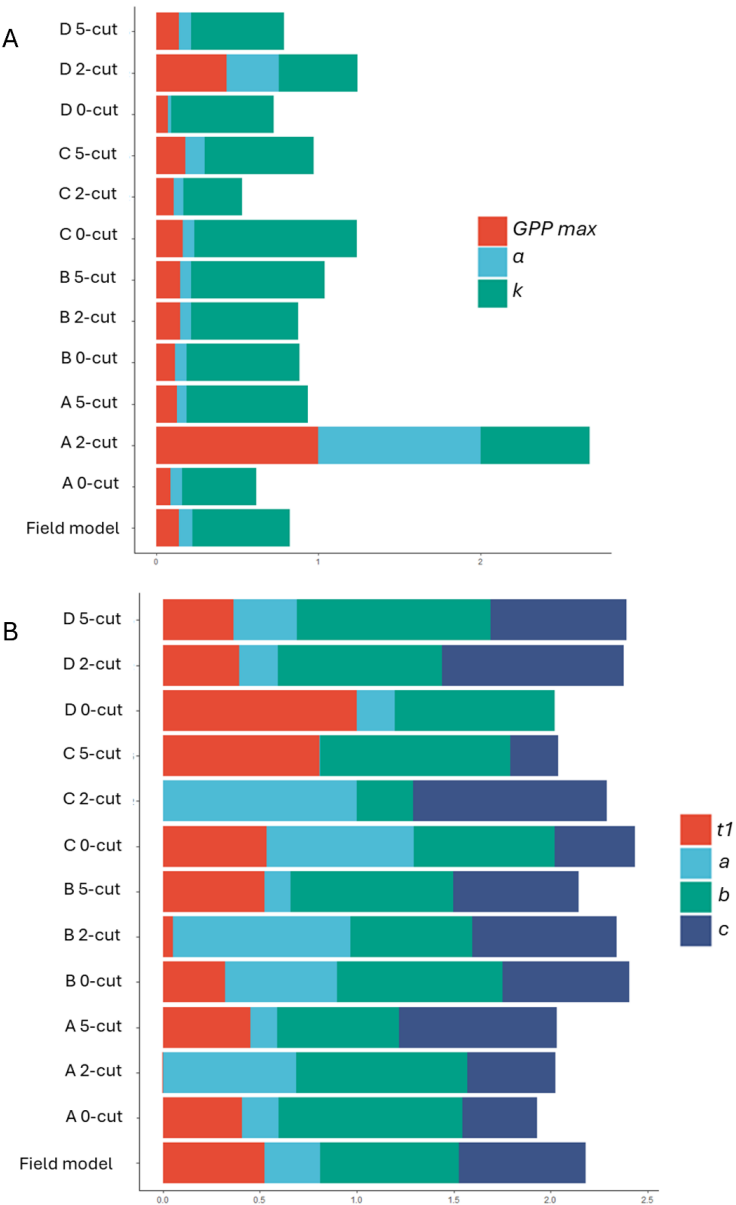
Block	Treatment	Model 2				Model 3				Model 4			
		R ²	NRMSE	NSE	AICc	R ²	NRMSE	NSE	AICc	R ²	NRMSE	NSE	AICc
A	0	0.95	21.4	0.95	980	0.96	19.4	0.96	1216	0.97	16.7	0.97	943
	2	0.85	39.2	0.84	1090	0.7	54.7	0.7	1424	0.88	34.8	0.88	1073
	5	0.71	53.5	0.71	1247	0.84	39.9	0.84	1481	0.82	42.5	0.82	1211
B	0	0.95	21.6	0.95	1029	0.93	26	0.93	1331	0.98	15.4	0.98	978
	2	0.71	53.3	0.71	1261	0.67	57.4	0.67	1570	0.74	50.7	0.74	1255
	5	0.83	40.7	0.83	1113	0.85	39	0.85	1389	0.85	38.3	0.85	1106
C	0	0.96	19.3	0.96	1109	0.92	27.7	0.92	1446	0.96	18.7	0.96	1106
	2	0.77	47.8	0.77	1175	0.71	53.8	0.71	1565	0.81	43.9	0.8	1163
	5	0.84	39.6	0.84	1227	0.84	39.9	0.84	1519	0.84	39.6	0.84	1229
D	0	0.9	32.1	0.9	1030	0.87	36.4	0.87	1348	0.9	32.1	0.9	1032
	2	0.82	41.8	0.82	1229	0.81	43.3	0.81	1533	0.88	34.3	0.88	1198
	5	0.91	31.1	0.9	1153	0.84	40.1	0.84	1484	0.92	28.5	0.92	1142

A, B, C, and D are the four blocks, The three harvest treatments at each block (plots) are 0, 2, and 5. The four indexes of model evaluation are: R^2 , normalized root mean square of error (NRMSE), Nash-Sutcliffe efficiency (NSE), and corrected Akaike information criterion (AICc).



328

329 Figure 4. Principal component analysis plots. PC1 vs PC2 (A), PC1 vs PC3 (B). Variability
330 explained by each PCA is the value in parenthesis. Colors represent the four studied blocks.
331 Harvest treatments are combined.



332
333 Figure 5. Variability of parameters fitted in R_{eco} model 4 (top) and the GPP model (bottom). Each
334 bar represents a plot, and the bottom bar corresponds to the pooled model. Each color
335 represents a different parameter. Parameter values were normalized i.e. dividing them by the
336 maximum value.

337
338



339 3.2 Carbon balance

340 Management had a marginally significant effect on GPP (p value < 0.1), with more negative
 341 GPP (highest photosynthesis) in the five-cut treatment ($-20.2 \pm 0.7 \text{ t CO}_2\text{-C ha}^{-1} \text{ yr}^{-1}$; mean \pm
 342 SE) and lowest in the 0-cut treatment ($-15.5 \pm 1.3 \text{ t CO}_2\text{-C ha}^{-1} \text{ yr}^{-1}$) (Table 3). No significant
 343 effects of management on R_{eco} (between 22.1 ± 2.5 and $22.4 \pm 3.3 \text{ t CO}_2\text{-C ha}^{-1} \text{ yr}^{-1}$; p value =
 344 0.98) and NEE (between 2.2 ± 0.5 and $6.9 \pm 2.2 \text{ t CO}_2\text{-C ha}^{-1} \text{ yr}^{-1}$; p value = 0.22) were
 345 registered although the NEE of 0-cut was $4.6 \text{ t CO}_2\text{-C ha}^{-1} \text{ yr}^{-1}$ higher than the two managed
 346 treatments on average. The 2-cut and 5-cut treatments gave similar annual biomass yields (4
 347 ± 0.7 and $4 \pm 0.2 \text{ t C ha}^{-1} \text{ yr}^{-1}$, respectively) leading to similar NECB for all treatments when
 348 the exported yields were added to the NEE (between 6.0 ± 0.5 and $6.9 \pm 2.2 \text{ t CO}_2\text{-C ha}^{-1} \text{ yr}^{-1}$
 349 ¹). Biomass yields of the 2-cut treatment were similar for both harvesting events, but much
 350 lower in block A compared to the other blocks, while for the 5-cut treatment yields peaked at
 351 the third harvest and were lowest at the fifth. There were less yield differences between
 352 blocks for the 5-cut treatment compared to the 2-cut treatment. Block D had the highest
 353 yields of both 2-cut and 5-cut treatments.

354 Although the experimental site looked rather uniform, large differences were seen between
 355 blocks, especially for R_{eco} and NEE, the latter with coefficients of variation of 0.56, 0.71,
 356 and 0.41, for the 0-cut, 2-cut, and 5-cut, respectively. The lowest R_{eco} was registered in block
 357 A, followed by block B, and the highest R_{eco} was in blocks C and D (p<0.05) (Table 3, Fig 6).
 358 Differences in GPP between blocks were not significant despite the higher GPP leading to
 359 lower biomass production in block A. Despite significant differences in R_{eco} , no significant
 360 difference in NEE was observed between blocks because the higher R_{eco} was accompanied by
 361 lower (more negative) GPP and thus higher biomass production. However, NECB was
 362 marginally different (p value < 0.1) between blocks, with lowest NECB in block A, followed



363 by block B, and highest in block C and D indicating that within field heterogeneity overrides
364 treatments. Figure 7 shows that the cumulative NEE grew faster in blocks C and D than in
365 blocks A and B leading to approximately eight times higher annual NEE in blocks C and D
366 compared to block A for the 0-cut treatment.

367 Cumulated methane emissions averaged $113 \text{ kg CH}_4 \text{ ha}^{-1} \text{ yr}^{-1}$ for the studied year and varied
368 primarily by block with less emissions at block C and largest emissions at block A (Table 4
369 and Fig. A2). Methane had no significant correlations with nutrients (Fig. A1), except NH_4 ,
370 which had a negative correlation with CH_4 . CH_4 also had a positive correlation with R_{eco} and
371 Ts but no significant correlation with WTD.



Table 3. Cumulated CO₂-C emission for the four studied blocks and harvest treatments during the study year.

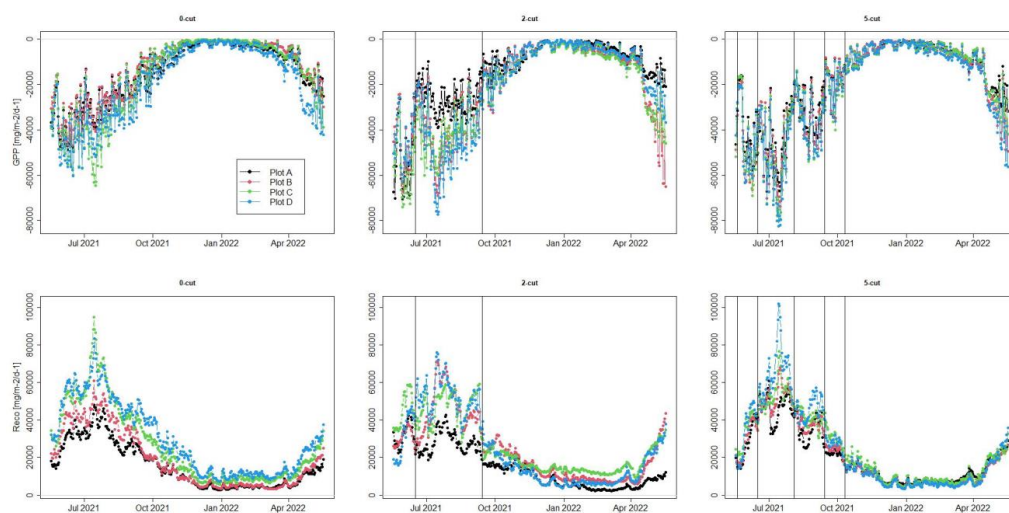
Block	Treatment	Reco	GPP	NEE	Yield	NECB
		t CO ₂ -C ha ⁻¹ yr ⁻¹	t CO ₂ -C ha ⁻¹ yr ⁻¹	t CO ₂ -C ha ⁻¹ yr ⁻¹	t C ha ⁻¹ yr ⁻¹	t C ha ⁻¹ yr ⁻¹
A	0-cut	15.4	-14.2	1.2	NA	1.2
B		18.6	-13	5.6	NA	5.6
C		26.2	-16	10.2	NA	10.2
D		29.4	-18.9	10.6	NA	10.6
Mean ± SE		22.4 ± 3.3	-15.5 ± 1.3	6.9 ± 2.2	NA	6.9 ± 2.2
A	2-cut	14.9	-15.3	-0.4	1.9	1.5
B		23.6	-20.8	2.8	4.5	7.3
C		26.4	-22	4.3	4.6	9
D		23.7	-20.6	3.1	5	8.1
Mean ± SE		22.1 ± 2.5	-19.7 ± 1.5	2.5 ± 1	4.0 ± 0.7	6.5 ± 1.7
A	5-cut	20.6	-18.5	2.2	3.5	5.6
B		21	-20.2	0.8	3.9	4.7
C		23.7	-20.4	3.3	3.5	6.8
D		24.3	-21.9	2.4	4.5	6.9
Mean ± SE		22.4 ± 0.9	-20.2 ± 0.7	2.2 ± 0.5	3.8 ± 0.2	6.0 ± 0.5

374

375 R_{eco} is ecosystem respiration, GPP is gross primary productivity, NEE is net ecosystem
 376 exchange, and NECB is net ecosystem carbon balance (NEE + yield).



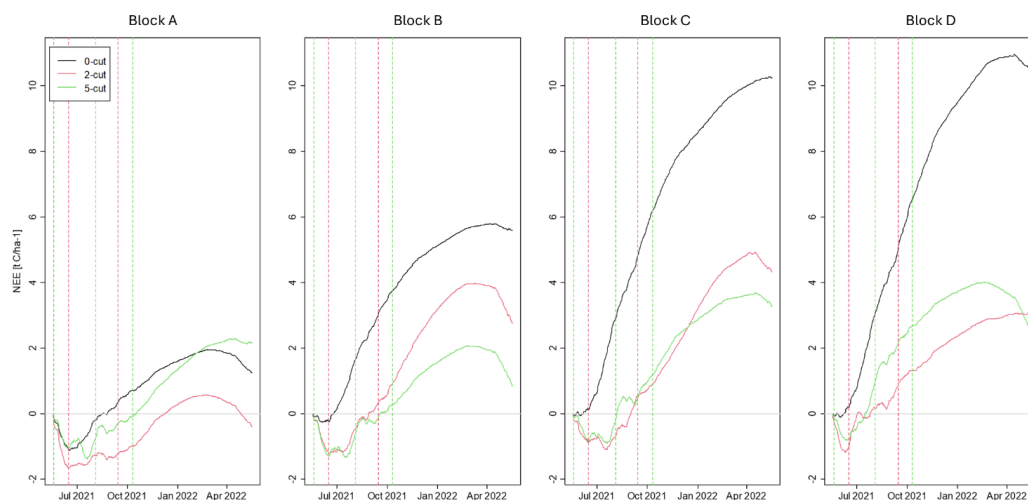
377



378

379 Figure 6. Modelled daily gross primary productivity (GPP) (top) and ecosystem respiration
 380 (R_{eco}) (bottom) for the three management treatments (0-cut, 2-cut, and 5-cut). Colors indicate
 381 the four block replicates. Vertical lines are harvesting events.

382



383

384 Figure 7. Cumulative net ecosystem exchange for the four studied blocks and three harvest
 385 treatments. Black line is the 0-cut, red line is the 2-cut, and green line is the 5-cut.
 386 Vertical green dashed lines are harvest events for only the 5-cut treatment while red dashed
 387 lines are harvest events for both the 2-cut and 5-cut treatments.

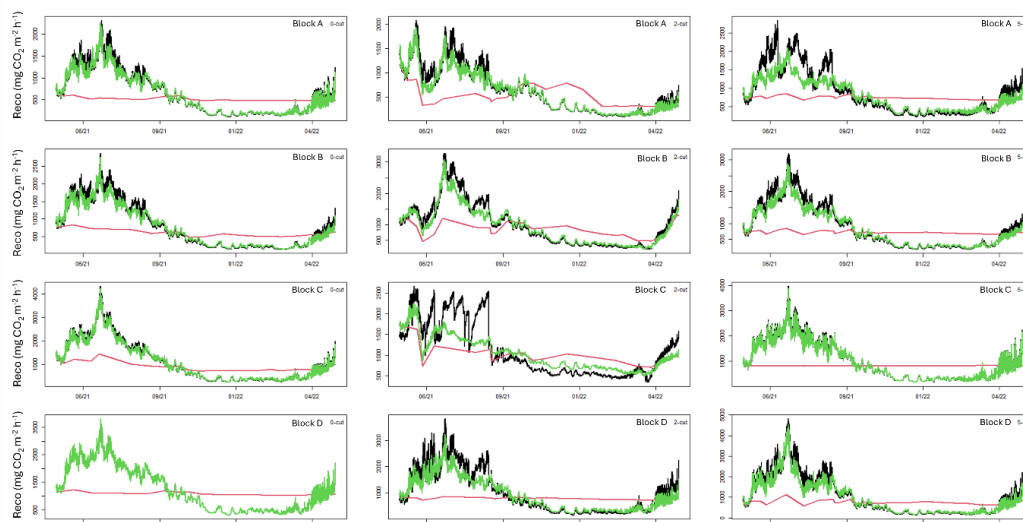


Table 4. Cumulated methane emissions for the blocks (A, B, C, D) and harvest treatments 0-cut, 2-cut, and 5-cut during the study year.

Block	Treatment	CH ₄ emissions
		kg CH ₄ ha ⁻¹
A	0-cut	200.2
	2-cut	157.5
	5-cut	125.7
	mean ± SD	161.1 ± 30.5
B	0-cut	124.0
	2-cut	129.0
	5-cut	99.4
	mean ± SD	117.5 ± 12.9
C	0-cut	35.7
	2-cut	40.1
	5-cut	73.7
	mean ± SD	49.8 ± 17
D	0-cut	114.5
	2-cut	190.0
	5-cut	67.6
	mean ± SD	124.0 ± 50.4
Total mean		113.1

3.3 Sensitivity analysis using WTD with different temporal resolution

Using annual mean WTD and annual mean Ts as input data for model 4 instead of hourly values, while keeping hourly RVI, underestimated R_{eco} between 9 to 26% for all plots with an average of 18% (Fig 8) (Table A4). On the other hand, using the annual mean WTD along with hourly Ts and RVI generally followed similar trends in R_{eco} as using hourly WTD as input data, but high emission events were slightly underestimated resulting in an underestimation that ranged between 0 and 10% with an average of 5% for all plots when compared to the model using hourly WTD, Ts, and RVI (Fig 8) (Table A4). If these R_{eco} values would be included in the CO₂ budget, this would result in a total mean NECB of 2.6 and 5.3 t C ha⁻¹ yr⁻¹, respectively.



401

402 Figure 8. Sensitivity of ecosystem respiration (R_{eco}) modelled for all plots to the data
 403 frequency of water table depth (WTD). Black lines represent R_{eco} modelled with hourly
 404 WTD, soil temperature (T_s), and RVI, green line represents R_{eco} modelled with mean annual
 405 WTD, hourly T_s , and hourly RVI, and red line represents R_{eco} modelled with mean annual
 406 WTD, mean annual T_s , and hourly RVI.

407 3.4 Water chemistry

408 The PCA described in total 67.8 % of the variance in data by the first three principal
 409 components. PC1 and PC2 explained 29.9 and 24.7% of the variability in the data,
 410 respectively, while PC3 explained 13.4% of the variability (Fig 4). The PC1 VS PC2 plot
 411 shows clustering of the data with blocks D and A having the largest difference. PC1 describes
 412 the pore water nutrients, which are positively correlated with each other, and significance of
 413 correlations are presented in Figure A1. This shows that WTD had positive correlations with
 414 Fe, TOC and DOC and negative correlations with NH_4 and TDP, while T_s had negative
 415 correlations with all nutrients except NH_4 and TDP. Predominant correlations of nutrients
 416 with R_{eco} were negative and positive with GPP and NEE, respectively.

417 Comparisons of water chemistry parameters between blocks indicated significant differences
 418 depending on type of nutrients. Generally, block (A) had the lowest nutrient concentrations,



419 while block (D) had the highest nutrient concentrations, with the exception of DOC. The
420 nutrient concentrations at the ditch appeared lower than the concentrations in the soil pore
421 water at the blocks except for the TP and TDP (Table 5). Comparisons between harvest
422 treatments showed that 2 and 5-cut treatments had higher N and Fe concentrations than the 0-
423 cut treatment, while there were no differences in other nutrients (Table 5). Additionally, the
424 interaction between harvest treatment and block was significant for NH_4 , electroconductivity,
425 pH, and turbidity.

426 The linear mixed model (Model 5) indicated that all nutrient concentrations, except NH_4 ,
427 significantly improved the base R_{eco} model (Table 6), however the effect of TP, TDP, and pH
428 also varied at plot level. For GPP, the addition of nutrients did not improve the base models,
429 however pH and EC improved model 6 with its effect varying at plot level. The magnitude of
430 model improvement (higher R^2 and lower RMSE) was larger for R_{eco} than for GPP, however,
431 in general the R^2 and RMSE did not change considerably for all nutrients/parameters
432 compared to the base models (Table A5).

433 Table 5. Mean annual concentrations of water chemistry parameters at block A, B, C, and D,
434 and treatments 0-cut, 2-cut, and 5-cut.

Block	pH	EC	Turbidity	TOC	DOC	TN	TDN	$\text{NH}_4\text{-N}$	$\text{NO}_3\text{-N}$	TP	TDP	Fe
		mS cm^{-1}	NTU	mg L^{-1}	mg L^{-1}	mg L^{-1}	mg L^{-1}	mg L^{-1}	mg L^{-1}	mg L^{-1}	mg L^{-1}	mg L^{-1}
A	5.61 ± 0.05 (a)	0.19 ± 0.01 (a)	25.4 ± 2.01 (ab)	164 ± 9 (a)	129 ± 7 (a)	14.1 ± 0.9 (a)	12.8 ± 0.8 (a)	1.56 ± 0.25 (a)	4.98 ± 3.18	0.49 ± 0.04 (a)	0.40 ± 0.04 (a)	12.2 ± 0.9 (a)
B	6.40 ± 0.04 (c)	0.34 ± 0.01 (c)	29.6 ± 2.95 (b)	212 ± 7 (b)	160 ± 5 (b)	16.8 ± 0.4 (b)	15.5 ± 0.5 (b)	1.50 ± 0.15 (a)	1.38 ± 0.58	0.81 ± 0.04 (c)	0.69 ± 0.05 (b)	22.9 ± 1.1 (b)
C	6.22 ± 0.04 (b)	0.34 ± 0.01 (b)	40.3 ± 3.76 (c)	193 ± 10 (b)	135 ± 6 (ab)	18.6 ± 0.9 (b)	16.2 ± 0.7 (b)	3.34 ± 0.29 (b)	2.97 ± 1.49	0.68 ± 0.04 (b)	0.50 ± 0.03 (a)	19.0 ± 1.6 (b)
D	6.25 ± 0.04 (b)	0.32 ± 0.01 (b)	26.7 ± 3.85 (a)	209 ± 16 (b)	137 ± 8 (a)	19.6 ± 1.2 (b)	18.9 ± 1.2 (b)	2.95 ± 0.24 (b)	3.58 ± 1.90	1.07 ± 0.08 (c)	0.91 ± 0.08 (b)	36.3 ± 3.6 (c)
ditch	6.65 ± 0.07	0.32 ± 0.01	41.9 ± 32.9	66 ± 8	42 ± 3	7.2 ± 1.8	4.6 ± 0.3	1.2 ± 0.2	1.09 ± 0.21	1.13 ± 0.23	0.93 ± 0.2	3.9 ± 1.1
Treatment												
0	6.13 ± 0.05 (b)	0.26 ± 0.01 (a)	27.3 ± 2.4	191 ± 9	137 ± 5	16.0 ± 0.8 (a)	14.5 ± 0.7 (a)	1.96 ± 0.16 (a)	0.15 ± 0.03	0.83 ± 0.06	0.63 ± 0.05	20.3 ± 1.9 (a)
2	6.04 ± 0.05 (a)	0.31 ± 0.01 (b)	33.3 ± 3.0	189 ± 10	136 ± 6	18.5 ± 0.9 (b)	16.9 ± 0.9 (b)	2.69 ± 0.30 (b)	7.49 ± 2.64	0.71 ± 0.04	0.59 ± 0.05	23.3 ± 1.9 (b)
5	6.20 ± 0.04 (b)	0.33 ± 0.01 (c)	30.5 ± 3.1	203 ± 10	148 ± 6	17.3 ± 0.7 (ab)	16.1 ± 0.7 (ab)	2.36 ± 0.18 (ab)	1.87 ± 0.49	0.76 ± 0.05	0.63 ± 0.05	24.3 ± 2.2 (ab)

435



436 Total organic carbon (TOC), dissolved organic carbon (DOC), total nitrogen (TN), total
437 dissolved nitrogen (TDN), ammonia (NH₄-N), nitrate (NO₃-N), total phosphorus (TP), total
438 dissolved phosphorus (TDP), electrical conductivity (EC). Values are means ± standard error.
439 Letters in parenthesis indicate significant differences between Blocks (top) and harvest
440 treatments (bottom). The ditch was not included in statistical comparisons. No comparisons
441 were performed with NO₃ due to insufficient data.

442

443 Table 6. Effect of soil pore water chemistry parameters on ecosystem respiration (R_{eco}, model
444 5) and gross primary productivity (GPP, model 6).

W.C. Parameter	R _{eco} effect	GPP effect
TOC	Sig	N
DOC	Sig	N
TN	Sig	N
TDN	Sig	N
NH ₄	N	N
TP	Sig*	N
TDP	Sig*	N
Fe	Sig*	N
pH	Sig*	Sig*
Turbidity	N	N
EC	N	Sig*

445

446 Sig indicates significant improvement of the models by individually adding water chemistry
447 parameters. Sig* indicates a significant effect that varied between harvest treatments. Water
448 chemistry parameters included total organic carbon (TOC), dissolved organic carbon (DOC),
449 total nitrogen (TN), total dissolved nitrogen (TDN), total phosphorus (TP), total dissolved
450 phosphorus (TDP), and electrical conductivity (EC).

451

452 4. Discussion

453 4.1 Management effect on C emissions

454 Comparison of results from this study to previous flux measurements on managed Danish

455 peatlands presented by Koch et al. (2023) shows that the total mean CO₂-C emissions

456 (NECB) from this study (6.5 t CO₂-C ha⁻¹ yr⁻¹) are larger than emissions from other Danish

457 organic soils at similar WTD (between 0 and 2.5 t CO₂-C ha⁻¹ yr⁻¹; Koch et al., 2023).

458 Similarly, our NECB is larger than emissions from peatlands under drained and rewetted

459 conditions at similar WTD from both Germany (between -1.0 t CO₂-C ha⁻¹ yr⁻¹ and 1.5 t CO₂-



460 C ha⁻¹ yr⁻¹; Tiemeyer et al., 2020) and the UK (between -2.0 t CO₂-C ha⁻¹ yr⁻¹ and 0.8 t CO₂-C
461 ha⁻¹ yr⁻¹; Evans et al., 2021). Our NECB results are closer to the lower range of emissions
462 from drained agricultural peatland presented by Koch et al. (2023). Nielsen et al. (2024)
463 reported the effect of management on GHG emissions from 2020 to 2021 at the same study
464 site as reported here, and found a higher mean NECB of 9.4 t CO₂-C ha⁻¹ yr⁻¹ at the slightly
465 lower mean annual WTD of -10 cm. Although mean annual WTD increased only 2 cm,
466 blocking of the drainage ditches resulted in considerably higher WTD during summer 2021
467 envisaged by temporary flooded conditions which could explain the lower NECB in 2021-22
468 compared to 2020-21 (Fig 2A). Other studies have also shown a delay in reaching carbon
469 neutral conditions despite drainage being stopped (Hemes et al., 2019; Kreyling et al., 2021).
470 For the shallow annual mean WTD registered at our study site we expected lower CO₂
471 emission according to IPCC Tier 1 emission factors. However, here R_{eco} is likely driven by
472 the dynamic interaction of a drop in WTD during summer coinciding with maximum Ts. This
473 naturally stimulated CO₂ production in the peat and together with plant respiration drove the
474 high annual R_{eco} (Fig 6).

475 Rewetted nutrient-rich fen peatlands have higher CO₂ emissions compared to low-nutrient
476 ones (Wilson et al., 2016). Management alternatives to reduce emissions from these sites are
477 therefore needed in order to meet emission reduction targets. Paludiculture has been found to
478 effectively reduce emissions from rewetted peatlands (Tanneberger et al., 2020; De Jong et
479 al., 2021; Bockermann et al., 2024). Our results showed that after three years of
480 establishment and management of RCG, NECB was not significantly different compared to
481 no management. These results support findings by Nielsen et al. (2024) who found no effect
482 of management on GHG emissions during the second year (2020) after RCG establishment at
483 the study site. The NECB assumes that all harvested biomass is converted to CO₂ when
484 removed from the field. However, if the biomass is considered as a resource potentially



485 reducing the use of fossil fuels, comparison of NEE among treatments would also be a
486 relevant measure. Based on NEE, we found a potential emission reduction of 4.5 and 4.7 t
487 CO₂-C ha⁻¹ yr⁻¹ for the 2 and 5-cut management strategies, respectively, in comparison to no
488 management, but this difference was not significant because of large variation between
489 treatment replicates especially for the 0-cut. Our NEE estimates were lower for all treatments
490 compared to Nielsen et al. (2024). We attribute this reduction in net CO₂ emissions not only
491 to the reduction in biomass production but also to the rewetting process, which lowered
492 heterotrophic peat mineralization. Considering the differences between the studied blocks
493 (treatment replicates), the potential reduction in CO₂ emission was larger in higher emission
494 areas, which in this study were also the areas with higher porewater nutrient concentrations.
495 In high emission areas, we found a potential reduction of up to 8.2 t CO₂-C ha⁻¹ yr⁻¹ (block D,
496 5-cut treatment) based on NEE and 3.7 t CO₂-C ha⁻¹ yr⁻¹ based on NECB. However, in areas
497 of less emissions (block A in this study), harvest of the biomass could not be recommended as
498 no benefit was seen. These results stress the importance of acknowledging peatland
499 heterogeneity in rewetting projects to maximize emission reductions.

500 A life cycle assessment of RCG on fen peatlands by Thers et al. (2023) showed that fuel
501 consumption during harvesting can make up a considerable amount of GHG emissions
502 associated to management. Since no considerable difference in yields were found between the
503 2-cut and 5-cut treatments, and a progressive decline was seen after the third harvest of the 5-
504 cut treatment, we would recommend the 2-cut management for RCG in peatlands such as the
505 study site to maximize harvest efficiency and to minimize disturbance to the peatland.
506 Although yields of 2021 (8.9 and 8.6 t DM ha⁻¹) (Table A1) were acceptable they were
507 considerably lower compared to 2019 yields (15.6 and 14.9 t DM ha⁻¹) (Nielsen et al., 2021)
508 and to 2020 yields (12.7 and 13.8 t DM ha⁻¹) (Nielsen et al., 2023a) for the 2-cut and the 5-
509 cut, respectively. The amount of N removed in the harvested biomass was on average 206 kg



510 N ha⁻¹ and slightly lower in the 2-cut compared to the 5-cut (Table A2), therefore, the same
 511 amount of N applied as fertilizer was removed at harvest. However, we found generally
 512 higher concentrations of N forms in pore water at the 2 and 5-cut treatments compared to the
 513 0-cut treatment. A complete assessment of the N balance would help to determine the full
 514 environmental benefit of RCG as paludiculture.

515 Mean CH₄ emissions from this study were within the range of emissions from other Danish
 516 and German peatlands reported by Koch et al. (2023) and Tiemeyer et al. (2020) and no
 517 treatment effect was apparent. We found that CH₄ emissions contributed 11.3% to total net
 518 mean NECB expressed as CO₂e (using GWP = 27 for CH₄). Peatland rewetting is expected to
 519 reduce CO₂ emissions while simultaneously increasing CH₄ emissions (Abdalla et al., 2016;
 520 Darusman et al., 2023). Thus, further monitoring of CH₄ emissions would be needed as
 521 rewetting progresses at the study site.

522 **4.2 Peatland heterogeneity**

523 Even though the studied area was relatively small (3.9 ha) and appeared to be uniform, we
 524 found differences in CO₂ emissions and porewater nutrients among the studied blocks, and
 525 preliminary peat chemistry data (Table 1) indicated some differences in pH, organic matter
 526 content, and TC among the studied blocks which might be due to the peat forming process.

527 Peatlands can be heterogeneous due to topography, groundwater flow, and vegetational
 528 variability, which can produce differences within peatlands in GHG emissions, pore water
 529 nutrient concentrations, and microbial communities (Arsenault et al., 2019; Chronakova et
 530 al., 2019; Kou et al., 2020). Fen peatlands in particular, have considerable heterogeneity with
 531 variable rates of peat and C accumulation (Piilo et al., 2020), and R_{eco} (Juszcak et al., 2013).
 532 Mashadi et al. (2024) found an increasing degree of peat decomposition at the study site
 533 approaching the stream, therefore, higher nutrient concentrations at blocks closer to the



stream could be explained by higher peat decomposition and organic matter mineralization at this area. Heterogeneity at the study site could also be seen by considerable variability in values of the fitted parameters of the R_{eco} and GPP models (Fig 5). Pooling all data to obtain field R_{eco} and GPP models resulted in lower model efficiencies (Table A6) compared to the approach of modelling each plot separately and led to similar R_{eco} , GPP, and NEE among treatments and blocks (Table A7). Higher model efficiencies and a better representation of CO_2 emissions from rewetted peatlands can be obtained by considering heterogeneity in these estimations.

4.3 Sensitivity to temporal resolution of WTD for prediction of R_{eco}

In previous studies, mean annual WTD have been used as the only predictor for NECB, but not without considerable variation in data points used to build these relationships (Tiemeyer et al., 2020; Evans et al., 2021; Koch et al., 2023). We found that information on Ts, RVI and PAR improved prediction as they have large impact on GPP and R_{eco} . Out of the three R_{eco} models we tested, the combined model including RVI, WTD and Ts performed best (model 4). When R_{eco} was estimated by models 2 or 3, where either RVI or WTD was omitted the annual R_{eco} and thus NECB was underestimated by 0.6 and 0.2 t C ha⁻¹ yr⁻¹, respectively. Therefore, model selection is important to accurately estimate CO_2 emissions from peatlands. The other two models evaluated (models 2 and 3) included Ts as explanatory variable. Temperature is a major soil respiration driver (Silvola et al., 1996; Lafleur et al., 2005; Rigney et al., 2018). Higher soil temperatures increase microbial activity and soil respiration. Soil respiration response to temperature changes, however, depend also on water table and soil moisture (Silvola et al., 1996; Lafleur et al., 2005).

In this study, Ts captured major trends in R_{eco} . This can be seen by the importance of the fitted Ts parameter (b , model 4) (Fig 5) and by results shown in Figure 8, in which hourly Ts



558 along with mean annual WTD captured most R_{eco} trends, However, this model underestimates
559 R_{eco} by an average of 5%, which would be equivalent to an NECB underestimation of 1.2 t C
560 $ha^{-1} yr^{-1}$ compared to the model with hourly WTD and hourly Ts. The use of mean annual
561 WTD and mean annual Ts would result in an even larger NECB underestimation (3.9 t C ha^{-1}
562 yr^{-1}) compared to the hourly model. This underestimation is due to the combined effect of
563 lower WTD and higher Ts during summer, dominates R_{eco} , and this is not captured when
564 mean WTD and Ts are used. These results showed the importance of using either high
565 temporal resolution WTD or Ts data, if available, to improve R_{eco} and NECB estimates from
566 rewetting peatlands. The model based on hourly WTD and Ts also improved simulation of
567 R_{eco} peaks (Fig 8), which might be of great importance under extreme weather and climate
568 change conditions. Juszczak et al (2013) also found that the response of R_{eco} to Ts can be
569 influenced by WTD and that models including both WTD and Ts provide a better
570 representation of R_{eco} in heterogeneous peatlands. Emission factors derived from models
571 based on annual mean WTD, such as those currently used for rewetted peatlands would
572 underestimate R_{eco} when applied to peatlands with fluctuating and lower WTD during the
573 warm season. This is an important observation particularly for rewetted peatlands, which
574 might take years to achieve hydrological stability (Kreyling et al., 2021). Improved CO_2
575 modelling therefore requires information on fluctuating WTD possibly obtained from
576 hydrological modelling if measurement data are unavailable.

577 **4.4 Effect of nutrients in CO_2 emissions**

578 Positive correlations between porewater nutrients suggest common drivers for their release.
579 Concentrations of dissolved organic matter components have been found to correlate with
580 concentrations of metals in Canadian bogs (Bourbonniere, 2009). Peat mineralization has
581 been found to be a major driver of nutrient release from drained peatlands (Cabezas et al.,
582 2013; Haapalehto et al., 2014). Predominantly higher nutrient concentrations at the studied



583 blocks compared to the ditch indicate differences between the pore water (measured at the
 584 plots) and the groundwater (measured at the ditch), suggesting that peat mineralization is the
 585 major pore water nutrient source. Peat nutrient concentrations and pH have been found to be
 586 potential indicators for GHG emissions in rewetting peatlands (Nielsen et al., 2023b). We
 587 showed that the prediction of R_{eco} was improved when soil pore water chemistry data were
 588 included in addition to WTD, RVI and T_s as fixed factors. Although, the magnitude of this
 589 improvement was small based on the R^2 increase, it indicated a relation between
 590 mineralization and porewater nutrients at the study site. The exact influence of nutrients in
 591 R_{eco} should be further investigated. In this study we measured nutrient concentrations but not
 592 nutrient load, which is the total mass of a nutrient and can be more informative about the
 593 nutrient status of the peatland (Cabezas et al., 2013). Under higher (shallower) WTD, nutrient
 594 concentrations can be diluted (Griffiths et al., 2019), Minor differences in WTD between the
 595 studied blocks could produce different degree of exposure to incoming water sources and
 596 explain lower nutrient concentrations at block A. Positive correlations between WTD and
 597 TOC, DOC and Fe could be due to release of DOC accumulated under drained summer
 598 conditions and increase in Fe solubility under higher water tables (Haapalehto et al., 2014).

599 Previous studies have explored variability on water chemistry between and within peatlands
 600 (Bourbonniere, 2009; Wood et al., 2016; Arsenault et al., 2018; Griffiths et al., 2019).

601 Nutrient concentrations in peatland's porewater are affected by several factors including
 602 water table depth, temperature, peat decomposition degree, and redox (Bourbonniere, 2009;
 603 Cabezas et al., 2013; Haapalehto et al., 2014; Wood et al., 2016). For this study, WTD was
 604 generally lower in blocks C and D (Fig 2B). Malinowski et al. (2015) found that the area
 605 where block A is located is more responsive to changes in the stream water level due to its
 606 proximity to the drainage ditch, which might have caused higher WTD at this block.

607 Additionally, differences in mobile porosity at the study site might have made some areas



608 more prone to be affected by changes in WTD than others (Mashadi et al., 2024). The minor
609 differences found in WTD might increase peat mineralization in drier blocks resulting in
610 higher DOC and N concentrations (Arsenault et al., 2018; Haapalehto et al., 2014; Wood et
611 al., 2016). Higher mineralization from block D was also evidenced by higher R_{eco} found in
612 this block. Higher plant productivity and fresh decomposable organic matter contributes to
613 higher nutrients found in rewetted peatlands (Haapalehto et al., 2014), which could explain
614 higher N concentrations found in blocks C and D. This is also supported by marginally higher
615 ($p < 0.1$) NECB found in these blocks compared to blocks A and B. A feedback mechanism
616 by which higher mineralization and nutrient release enhances plant productivity, which in
617 turn increases fresh organic matter inputs into the soil and further nutrient releases could
618 drive high nutrient concentrations in poorly drained fen peatlands such as this one.

619 **4.5 Considerations for the potential use of RCG harvested biomass**

620 In order to reestablish the C sink function of rewetted peatlands, peat formation would need
621 to be reestablished, however, reaching this state may take decades (Kreyling et al., 2021).
622 Through replacing the use of fossil fuels, paludiculture provides an opportunity for achieving
623 an indirect emission reduction, since harvested biomass C makes out a considerable amount
624 of GHG emissions from cultivated RCG in fen peatlands (Thers et al., 2023). The end use of
625 the harvested biomass is key to achieve the potential GHG mitigation. Reed canary grass
626 grown in wet Danish fen peatlands was shown suitable for protein extraction as supplement
627 in the diets of monogastric animals and side streams or all the harvested biomass could be
628 used for biogas production thereby replacing fossil fuels (Kandel et al., 2013; Nielsen et al.
629 2021; Nielsen et al., 2023a). The feasibility of using biomass from reed canary grass to offset
630 fossil fuels would depend on the development of non-invasive harvesting techniques, the
631 identification of viable and economically suitable uses for this biomass, and the establishment
632 of markets and infrastructure for its processing.



633

634 **5. Conclusion**

635 We found that harvesting moderately fertilized RCG in the third production year did not
636 increase net C emissions significantly in poorly drained fen peatlands compared to no
637 management. Additionally, the NECB was reduced further under management compared to
638 previous years as rewetting progressed, and a biomass resource that potentially could reduce
639 GHG emission elsewhere depending on the end use was produced. Considering the
640 heterogeneity of the field, results also indicated that harvest of the biomass only reduced net
641 C fluxes at nutrient rich areas. At relatively nutrient poor areas it seems more advantageous to
642 leave the grass without management. Paludiculture and management of RCG in rewetting fen
643 peatlands, therefore, offers an alternative that could be particularly beneficial in high nutrient
644 rich areas. We found that differences in annual NECB were highly influenced by R_{eco} , and
645 that R_{eco} was best modelled by daily data on RVI, WTD and Ts, with R_{eco} being
646 underestimated when the mean WTD was used instead of hourly values, indicating that
647 temporal variability in WTD should be considered in establishing emission factors for
648 rewetted fen peatlands. Differences in porewater nutrient concentrations were able to further
649 improve prediction of R_{eco} based on a statistical model. As more nutrients could be related to
650 higher CO₂ emissions, we suggest a feedback mechanism driving the mineralization, nutrient
651 release, biomass production and peatland heterogeneity. Further research and the
652 establishment of infrastructure and markets for harvested biomass would improve the
653 prospects of paludiculture in rewetted peatlands.

654

655 **Competing interests**

656 The authors declare that they have no conflict of interest.



657

658 **Acknowledgments**

659

660 The authors would like to acknowledge the following people from the Agroecology
 661 Department at Aarhus University, Viborg: Michael Koppelgaard for his help in data collection
 662 and processing, Maarit Mäenpää for her help in the statistical analyses, Claudia Nielsen for
 663 her help in data processing, and Kirsten Kørup for her help in biomass harvesting.

664 **Funding sources**

665 This study was part of the INSURE project that received funding from the European Joint
 666 Programme EJP Soil under the European Union's Horizon 2020 research and innovation with
 667 grant agreement no. 862695. Co-funding was received from RePeat DK funded by the Danish
 668 Agricultural Agency.

669

670 **References**

- 671 Abdalla, M., Hastings, A., Truu, J., Espenberg, M., Mander, Ü., & Smith, P. (2016).
 672 Emissions of methane from northern peatlands: a review of management impacts and
 673 implications for future management options. *Ecology and Evolution*, 6(19), 7080-7102.
- 674 AminiTabrizi, R., Dontsova, K., Grachet, N. G., & Tfaily, M. M. (2022). Elevated
 675 temperatures drive abiotic and biotic degradation of organic matter in a peat bog under oxic
 676 conditions. *Science of the Total Environment*, 804, 150045.
- 677 Andersen, R., Farrell, C., Graf, M., Muller, F., Calvar, E., Frankard, P., ... & Anderson, P.
 678 (2017). An overview of the progress and challenges of peatland restoration in Western
 679 Europe. *Restoration Ecology*, 25(2), 271-282.
- 680 Arsenault, J., Talbot, J., & Moore, T. R. (2018). Environmental controls of C, N and P
 681 biogeochemistry in peatland pools. *Science of the Total Environment*, 631, 714-722.
- 682 Arsenault, J., Talbot, J., Moore, T. R., Beauvais, M. P., Franssen, J., & Roulet, N. T. (2019).
 683 The spatial heterogeneity of vegetation, hydrology and water chemistry in a peatland with
 684 open-water pools. *Ecosystems*, 22, 1352-1367.



- 685 Best, E. K. (1976). An automated method for determining nitrate nitrogen in soil
686 extracts. *Queensland Journal of Agricultural and Animal Sciences*, 33, 161-166.
- 687 Bianchi, A., Larmola, T., Kekkonen, H., Saarnio, S., & Lång, K. (2021). Review of
688 greenhouse gas emissions from rewetted agricultural soils. *Wetlands*, 41, 1-7.
- 689 Bockermann, C., Eickenscheidt, T., & Drösler, M. (2024). Adaptation of fen peatlands to
690 climate change: rewetting and management shift can reduce greenhouse gas emissions and
691 offset climate warming effects. *Biogeochemistry*, 1-26.
- 692 Bourbonniere, R. A. (2009). Review of water chemistry research in natural and disturbed
693 peatlands. *Canadian water resources journal*, 34(4), 393-414.
- 694 Cabezas, A., Gelbrecht, J., Zwirnmann, E., Barth, M., & Zak, D. (2012). Effects of degree of
695 peat decomposition, loading rate and temperature on dissolved nitrogen turnover in rewetted
696 fens. *Soil Biology and Biochemistry*, 48, 182-191.
- 697 Cabezas, A., Gelbrecht, J., & Zak, D. (2013). The effect of rewetting drained fens with
698 nitrate-polluted water on dissolved organic carbon and phosphorus release. *Ecological
699 engineering*, 53, 79-88.
- 700 Chroňáková, A., Bárta, J., Kaštovská, E., Urbanová, Z., & Pícek, T. (2019). Spatial
701 heterogeneity of belowground microbial communities linked to peatland microhabitats with
702 different plant dominants. *FEMS Microbiology Ecology*, 95(9), 1-130.
- 703 Crooke, W. M., & Simpson, W. E. (1971). Determination of ammonium in Kjeldahl digests of
704 crops by an automated procedure. *Journal of the Science of Food and Agriculture*, 22(1), 9-
705 10.
- 706 Dansk Standard (2004) DS 291. Water Analyses – orthophosphate-phosphorus. Photometric
707 method.
- 708 Darusman, T., Murdiyarso, D., Impron, & Anas, I. (2023). Effect of rewetting degraded
709 peatlands on carbon fluxes: a meta-analysis. *Mitigation and Adaptation Strategies for Global
710 Change*, 28(3), 10.
- 711 de Jong, M., van Hal, O., Pijlman, J., van Eekeren, N., & Junginger, M. (2021). Paludiculture
712 as paludifuture on Dutch peatlands: An environmental and economic analysis of Typha
713 cultivation and insulation production. *Science of the Total Environment*, 792, 148161.
- 714 Dragoni, F., Giannini, V., Ragolini, G., Bonari, E., & Silvestri, N. (2017). Effect of harvest
715 time and frequency on biomass quality and biomethane potential of common reed
716 (*Phragmites australis*) under paludiculture conditions. *BioEnergy research*, 10, 1066-1078.
- 717 Elsgaard, L., Görres, C. M., Hoffmann, C. C., Blicher-Mathiesen, G., Schelde, K., &
718 Petersen, S. O. (2012). Net ecosystem exchange of CO₂ and carbon balance for eight
719 temperate organic soils under agricultural management. *Agriculture, ecosystems &
720 environment*, 162, 52-67.
- 721 Emsens, W. J., van Diggelen, R., Aggenbach, C. J., Cajthaml, T., Frouz, J., Klimkowska, A.,
722 ... & Verbruggen, E. (2020). Recovery of fen peatland microbiomes and predicted functional
723 profiles after rewetting. *The ISME journal*, 14(7), 1701-1712.



- 724 Erb, K. H., Kastner, T., Plutzer, C., Bais, A. L. S., Carvalhais, N., Fetzner, T., ... & Luyssaert,
725 S. (2018). Unexpectedly large impact of forest management and grazing on global vegetation
726 biomass. *Nature*, 553(7686), 73-76.
- 727 Evans, C. D., Peacock, M., Baird, A. J., Artz, R. R. E., Burden, A., Callaghan, N., ... &
728 Morrison, R. (2021). Overriding water table control on managed peatland greenhouse gas
729 emissions. *Nature*, 593(7860), 548-552.
- 730 Geurts, J. J., Oehmke, C., Lambertini, C., Eller, F., Sorrell, B. K., Mandiola, S. R., ... & Fritz,
731 C. (2020). Nutrient removal potential and biomass production by *Phragmites australis* and
732 *Typha latifolia* on European rewetted peat and mineral soils. *Science of the Total*
733 *Environment*, 747, 141102.
- 734 Giannini, V., Silvestri, N., Dragoni, F., Pistocchi, C., Sabbatini, T., & Bonari, E. (2017).
735 Growth and nutrient uptake of perennial crops in a paludicultural approach in a drained
736 Mediterranean peatland. *Ecological engineering*, 103, 478-487.
- 737 Görres, C. M., Kutzbach, L., & Elsgaard, L. (2014). Comparative modeling of annual CO₂
738 flux of temperate peat soils under permanent grassland management. *Agriculture, ecosystems*
739 *& environment*, 186, 64-76.
- 740 Griffiths, N. A., Sebestyen, S. D., & Oleheiser, K. C. (2019). Variation in peatland porewater
741 chemistry over time and space along a bog to fen gradient. *Science of the total*
742 *environment*, 697, 134152.
- 743 Haapalehto, T., Kotiaho, J. S., Matilainen, R., & Tahvanainen, T. (2014). The effects of long-
744 term drainage and subsequent restoration on water table level and pore water chemistry in
745 boreal peatlands. *Journal of Hydrology*, 519, 1493-1505.
- 746 Hartung, C., Andrade, D., Dandikas, V., Eickenscheidt, T., Drösler, M., Zollfrank, C., &
747 Heuwinkel, H. (2020). Suitability of paludiculture biomass as biogas substrate— biogas yield
748 and long-term effects on anaerobic digestion. *Renewable energy*, 159, 64-71.
- 749 Hemes, K. S., Chamberlain, S. D., Eichelmann, E., Anthony, T., Valach, A., Kasak, K., ... &
750 Baldocchi, D. D. (2019). Assessing the carbon and climate benefit of restoring degraded
751 agricultural peat soils to managed wetlands. *Agricultural and Forest Meteorology*, 268, 202-
752 214.
- 753 Jurasinski G, Koebisch F, Guenther A, Beetz S (2022). `_flux`: Flux Rate Calculation from
754 Dynamic Closed Chamber Measurements_. R package version 0.3-0.1, <[https://CRAN.R-](https://CRAN.R-project.org/package=_flux)
755 [project.org/package=_flux](https://CRAN.R-project.org/package=_flux)>.
- 756 Juszczak, R., Humphreys, E., Acosta, M., Michalak-Galczewska, M., Kayzer, D., & Olejnik,
757 J. (2013). Ecosystem respiration in a heterogeneous temperate peatland and its sensitivity to
758 peat temperature and water table depth. *Plant and Soil*, 366, 505-520.
- 759 Kandel, T. P., Sutaryo, S., Möller, H. B., Jørgensen, U., & Lærke, P. E. (2013). Chemical
760 composition and methane yield of reed canary grass as influenced by harvesting time and
761 harvest frequency. *Bioresource technology*, 130, 659-666.



- 762 Kandel, T. P., Elsgaard, L., & Lærke, P. E. (2017). Annual balances and extended seasonal
763 modelling of carbon fluxes from a temperate fen cropped to festulolium and tall fescue under
764 two-cut and three-cut harvesting regimes. *GCB Bioenergy*, 9(12), 1690-1706.
- 765 Kandel, T. P., Karki, S., Elsgaard, L., & Lærke, P. E. (2019). Fertilizer-induced fluxes
766 dominate annual N₂O emissions from a nitrogen-rich temperate fen rewetted for
767 paludiculture. *Nutrient Cycling in Agroecosystems*, 115, 57-67.
- 768 Kreyling, J., Tanneberger, F., Jansen, F., Van Der Linden, S., Aggenbach, C., Blüml, V., ... &
769 Jurasinski, G. (2021). Rewetting does not return drained fen peatlands to their old selves.
770 *Nature communications*, 12(1), 5693.
- 771 Koch, J., Elsgaard, L., Greve, M. H., Gyldenkerne, S., Hermansen, C., Levin, G., ... &
772 Stisen, S. (2023). Water table driven greenhouse gas emission estimate guides peatland
773 restoration at national scale. *Biogeosciences Discussions*, 2023, 1-28.
- 774 Kou, D., Virtanen, T., Treat, C. C., Tuovinen, J. P., Räsänen, A., Juutinen, S., ... & Shurpali,
775 N. J. (2022). Peatland heterogeneity impacts on regional carbon flux and its radiative effect
776 within a boreal landscape. *Journal of Geophysical Research: Biogeosciences*, 127(9),
777 e2021JG006774.
- 778 Lafleur, P. M., Moore, T. R., Roulet, N. T., & Frolking, S. (2005). Ecosystem respiration in a
779 cool temperate bog depends on peat temperature but not water table. *Ecosystems*, 8, 619-629.
- 780 Leifeld, J., & Menichetti, L. (2018). The underappreciated potential of peatlands in global
781 climate change mitigation strategies. *Nature communications*, 9(1), 1071.
- 782 Liu, H., Zak, D., Rezanezhad, F., & Lennartz, B. (2019). Soil degradation determines release
783 of nitrous oxide and dissolved organic carbon from peatlands. *Environmental Research*
784 *Letters*, 14(9), 094009.
- 785 Liu, W., Fritz, C., Weideveld, S. T., Aben, R. C., Van Den Berg, M., & Velthuis, M. (2022).
786 Annual CO₂ budget estimation from chamber-based flux measurements on intensively
787 drained peat meadows: Effect of gap-filling strategies. *Frontiers in Environmental*
788 *Science*, 10, 803746.
- 789 Loisel, J., & Gallego-Sala, A. (2022). Ecological resilience of restored peatlands to climate
790 change. *Communications Earth & Environment*, 3(1), 208.
- 791 Malinowski, R., Groom, G., Schwanghart, W., & Heckrath, G. (2015). Detection and
792 delineation of localized flooding from WorldView-2 multispectral data. *Remote*
793 *sensing*, 7(11), 14853-14875.
- 794 Mashhadi, S. R., Grombacher, D., Zak, D., Lærke, P. E., Andersen, H. E., Hoffmann, C. C., &
795 Petersen, R. J. (2024). Borehole nuclear magnetic resonance as a promising 3D mapping tool
796 in peatland studies. *Geoderma*, 443, 116814.
- 797 Nielsen, C. K., Stødkilde, L., Jørgensen, U., & Lærke, P. E. (2021). Effects of harvest and
798 fertilization frequency on protein yield and extractability from flood-tolerant perennial
799 grasses cultivated on a fen peatland. *Frontiers in Environmental Science*, 9, 619258.



- 800 Nielsen, C. K., Stødtkilde, L., Jørgensen, U., & Lærke, P. E. (2023a). Ratio vegetation indices
801 have the potential to predict extractable protein yields in green protein paludiculture. *Mires &*
802 *Peat*, (29).
- 803 Nielsen, C. K., Elsgaard, L., Jørgensen, U., & Lærke, P. E. (2023b). Soil greenhouse gas
804 emissions from drained and rewetted agricultural bare peat mesocosms are linked to
805 geochemistry. *Science of the Total Environment*, 896, 165083.
- 806 Nielsen, C. K., Liu, W., Koppelgaard, M., & Laerke, P. E. (2024). To Harvest or not to
807 Harvest: Management Intensity did not Affect Greenhouse Gas Balances of Phalaris
808 *Arundinacea* Paludiculture. *Wetlands*, 44(6), 79.
- 809 Page, S. E., & Baird, A. J. (2016). Peatlands and global change: response and
810 resilience. *Annual Review of Environment and Resources*, 41, 35-57.
- 811 Piilo, S. R., Korhola, A., Heiskanen, L., Tuovinen, J. P., Aurela, M., Juutinen, S., ... &
812 Välranta, M. M. (2020). Spatially varying peatland initiation, Holocene development, carbon
813 accumulation patterns and radiative forcing within a subarctic fen. *Quaternary Science*
814 *Reviews*, 248, 106596.
- 815 Purre, A. H., Penttilä, T., Ojanen, P., Minkkinen, K., Aurela, M., Lohila, A., & Ilomets, M.
816 (2019). Carbon dioxide fluxes and vegetation structure in rewetted and pristine peatlands in
817 Finland and Estonia. *Boreal Environment Research*.
- 818 Putkinen, A., Tuittila, E. S., Siljanen, H. M., Bodrossy, L., & Fritze, H. (2018). Recovery of
819 methane turnover and the associated microbial communities in restored cutover peatlands is
820 strongly linked with increasing Sphagnum abundance. *Soil Biology and Biochemistry*, 116,
821 110-119.
- 822 R Core Team (2023). *_R: A Language and Environment for Statistical Computing_*. R
823 Foundation for Statistical Computing, Vienna, Austria. <<https://www.R-project.org/>>.
- 824 Ren, L., Eller, F., Lambertini, C., Guo, W. Y., Brix, H., & Sorrell, B. K. (2019). Assessing
825 nutrient responses and biomass quality for selection of appropriate paludiculture
826 crops. *Science of the Total Environment*, 664, 1150-1161.
- 827 Scharlemann, J. P., Tanner, E. V., Hiederer, R., & Kapos, V. (2014). Global soil carbon:
828 understanding and managing the largest terrestrial carbon pool. *Carbon management*, 5(1),
829 81-91.
- 830 Silvola, J., Alm, J., Ahlholm, U., Nykanen, H., & Martikainen, P. J. (1996). CO₂ fluxes from
831 peat in boreal mires under varying temperature and moisture conditions. *Journal of ecology*,
832 219-228.
- 833 Rigney, C., Wilson, D., Renou-Wilson, F., Müller, C., Moser, G., & Byrne¹, K. A. (2018).
834 Greenhouse gas emissions from two rewetted peatlands previously managed for forestry.
835 *Mires and Peat*, 21, 1-23.
- 836 Song, Y., Cheng, X., Song, C., Li, M., Gao, S., Liu, Z., ... & Wang, X. (2022). Soil CO₂ and
837 N₂O emissions and microbial abundances altered by temperature rise and nitrogen addition in
838 active-layer soils of permafrost peatland. *Frontiers in Microbiology*, 13, 1093487.



- 839 Tanneberger, F., Schröder, C., Hohlbein, M., Lenschow, U., Permien, T., Wichmann, S., &
840 Wichtmann, W. (2020). Climate change mitigation through land use on rewetted peatlands–
841 cross-sectoral spatial planning for paludiculture in Northeast Germany. *Wetlands*, 40(6),
842 2309-2320.
- 843 Thers, H., Knudsen, M. T., & Lærke, P. E. (2023). Comparison of GHG emissions from
844 annual crops in rotation on drained temperate agricultural peatland with production of reed
845 canary grass in paludiculture using an LCA approach. *Heliyon*, 9(6).
- 846 Tiemeyer, B., Freibauer, A., Borraz, E. A., Augustin, J., Bechtold, M., Beetz, S., ... & Drösler,
847 M. (2020). A new methodology for organic soils in national greenhouse gas inventories: Data
848 synthesis, derivation and application. *Ecological Indicators*, 109, 105838.
- 849 Urbanová, Z., & Bárta, J. (2020). Recovery of methanogenic community and its activity in
850 long-term drained peatlands after rewetting. *Ecological engineering*, 150, 105852.
- 851 Vroom, R. J., Xie, F., Geurts, J. J., Chojnowska, A., Smolders, A. J., Lamers, L. P., & Fritz, C.
852 (2018). *Typha latifolia* paludiculture effectively improves water quality and reduces
853 greenhouse gas emissions in rewetted peatlands. *Ecological engineering*, 124, 88-98.
- 854 Wilson, D., Blain, D., Couwenberg, J., Evans, C. D., Murdiyarso, D., Page, S., ... & Tuittila,
855 E. S. (2016). Greenhouse gas emission factors associated with rewetting of organic soils.
856 *Mires and Peat*, 17, 1-28.
- 857 Wood, M. E., Macrae, M. L., Strack, M., Price, J. S., Osko, T. J., & Petrone, R. M. (2016).
858 Spatial variation in nutrient dynamics among five different peatland types in the Alberta oil
859 sands region. *Ecohydrology*, 9(4), 688-699.
- 860 Yu, Z., Loisel, J., Brosseau, D. P., Beilman, D. W., & Hunt, S. J. (2010). Global peatland
861 dynamics since the Last Glacial Maximum. *Geophysical research letters*, 37(13).
- 862 Zak, D., Roth, C., Unger, V., Goldhammer, T., Fenner, N., Freeman, C., & Jurasinski, G.
863 (2019). Unraveling the importance of polyphenols for microbial carbon mineralization in
864 rewetted riparian peatlands. *Frontiers in Environmental Science*, 7, 147.
- 865 Zambrano-Bigiarini, M. (2020) hydroGOF: Goodness-of-fit functions for comparison of
866 simulated and observed hydrological time series, R package version 0.4-0. URL
867 <https://github.com/hzambran/hydroGOF>. DOI:10.5281/zenodo.839854.
- 868 Zhong, Y., Jiang, M., & Middleton, B. A. (2020). Effects of water level alteration on carbon
869 cycling in peatlands. *Ecosystem Health and Sustainability*, 6(1), 1806113.
- 870 Ziegler, R. (2020). Paludiculture as a critical sustainability innovation mission. *Research*
871 *Policy*, 49(5), 103979.



872 **Appendix A**

873 Table A1. Biomass yields for each harvest event.

treatment	block	Yield per harvest event (t DM ha ⁻¹)					Total
		20-May	16-jun	04-Ago	14-sep	11-Oct	
2-cut	A	-	2.8	-	1.4	-	4.2
2-cut	B	-	5.3	-	4.8	-	10.1
2-cut	C	-	4.4	-	5.8	-	10.2
2-cut	D	-	4.6	-	6.5	-	11.1
5-cut	A	1.5	1.5	2.9	1.4	0.5	7.8
5-cut	B	1.0	2.6	3.0	1.7	0.5	8.7
5-cut	C	0.3	1.3	3.5	2.1	0.7	7.8
5-cut	D	1.2	1.9	4.2	2.0	0.7	10.1

874

875 Table A2. Total N in harvested biomass per event

treatment	block	total N in biomass per harvest event (kg ha ⁻¹)					Total
		20-May	16-jun	04-Ago	14-sep	11-Oct	
2-cut	A	-	62	-	31	-	93
2-cut	B	-	104	-	91	-	195
2-cut	C	-	99	-	116	-	215
2-cut	D	-	91	-	113	-	204
5-cut	A	49	38	56	40	21	204
5-cut	B	34	61	65	52	20	233
5-cut	C	13	35	93	74	31	245
5-cut	D	41	47	83	59	27	258

876

877

878

879

880

881

882

883

884

885

886

887

888



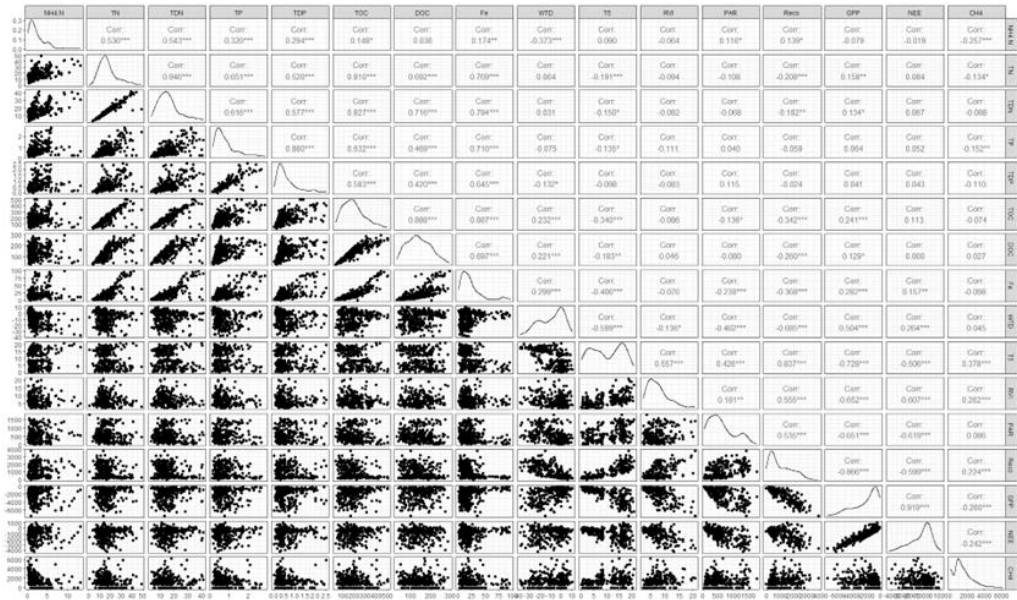
889 Table A3. Model evaluation for GPP model. Values are three different indexes of model
 890 performance for each block.

Block	Treatment	GPP model		
		R ²	NRMSE	NSE
A	0-cut	0.9	31.1	0.9
	2-cut	0.94	24.2	0.94
	5-cut	0.89	33.9	0.88
B	0-cut	0.91	29.9	0.91
	2-cut	0.96	19.3	0.96
	5-cut	0.94	24.4	0.94
C	0-cut	0.92	27.6	0.92
	2-cut	0.81	43.4	0.81
	5-cut	0.91	30.6	0.91
D	0-cut	0.86	37.5	0.86
	2-cut	0.91	29.3	0.91
	5-cut	0.9	32.4	0.89

891 A, B, C, and D are the four block replicates, The three harvest treatments at each block are 0,
 892 2, and 5. The three indexes of model evaluation are: R², normalized root mean square of error
 893 (NRMSE), and Nash-Sutcliffe efficiency (NSE).

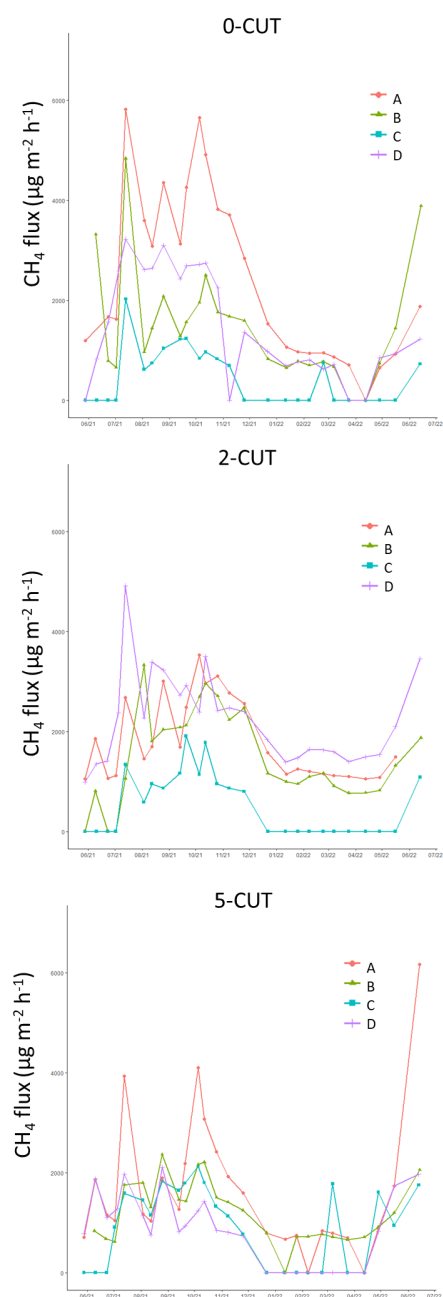


894 Figure A1. Pearson's correlations of water chemistry parameters, Ecosystem respiration
895 (R_{eco}), net ecosystem exchange (NEE), gross primary productivity (GPP), water table depth
896 (WTD), soil temperature at 5 cm depth (T_5), ammonia ($NH_4.N$), total nitrogen (TN), total
897 dissolved nitrogen (TDN), total phosphorus (TP), total dissolved phosphorus (TDP), total
898 organic carbon (TOC), and dissolved organic carbon (DOC). * significant at $p < 0.05$, **
899 significant at $0.01 > p > 0.001$ *** significant at $p < 0.001$





914 Figure A2. Time series of methane emissions from studied blocks (different line colors) and
915 from the three harvest treatments (zero cut, two cut, and five cut). Each dot in the lines
916 represents a measurement campaign. CH₄ emissions calculated only under 0% PAR
917 conditions.



918



919 Table A4. Comparison of annual R_{eco} estimated with models 4, 2 and 3, which use hourly data
920 on Ts, WTD and RVI, model 4 using either mean annual WTD and Ts (M Model), and model
921 4 using mean annual WTD and hourly Ts (MH model), the latter two models including hourly
922 RVI data.

923

Block	Treatment	Model 4	Model 2	Model 3	M model	MH model
		t CO ₂ -C ha ⁻¹ yr ⁻¹				
A	0	15.4	14.9	15.4	12.2	14.8
B		18.6	18.4	18.9	14.4	17.7
C		26.2	26.1	25.6	21.6	25.8
D		29.4	29.4	31	25.9	29.4
Average ± SE		22.4 ± 3.3	22.2 ± 3.4	22.7 ± 3.5	18.5 ± 3.2	21.9 ± 3.4
A	2	14.9	14.5	15.1	12.3	13.9
B		23.6	23.4	23.6	20.5	22.4
C		26.4	25.7	26	24.1	24.4
D		23.7	22.7	23	18.7	21.4
Average ± SE		22.1 ± 2.5	21.6 ± 2.4	21.9 ± 2.4	18.9 ± 2.5	20.6 ± 2.3
A	5	20.6	18.6	19.3	17.4	18.6
B		21	20.8	20.5	17.0	19.7
C		23.7	23.6	23.4	19.8	23.4
D		24.3	22.9	23.4	17.9	22.6
Average ± SE		22.4 ± 0.9	21.5 ± 1.1	21.7 ± 1	18 ± 0.6	21.1 ± 1.1

924



925 Table A5. Total organic carbon (TOC), dissolved organic carbon (DOC), total nitrogen (TN),
926 total dissolved nitrogen (TDN), total phosphorus (TP), total dissolved phosphorus (TDP),
927 Turbidity (NTU), electrical conductivity (EC). If base model did not improve by adding the
928 water chemistry parameters, R^2 and RMSE are not shown.

929

Parameter	Reco models				GPP models			
	Base R^2	Improved R^2	Base RMSE	Improved RMSE	Base R^2	Improved R^2	Base RMSE	Improved RMSE
TOC	0.863	0.873	243	226	-	-	-	-
DOC	0.863	0.871	242	228	-	-	-	-
TN	0.863	0.870	244	229	-	-	-	-
TDN	0.864	0.876	242	224	-	-	-	-
NH ₄	-	-	-	-	-	-	-	-
TP	0.867	0.871	241	231	-	-	-	-
TDP	0.862	0.867	244	229	-	-	-	-
FE	0.863	0.878	242	225	-	-	-	-
pH	0.863	0.868	243	239	0.832	0.839	645	628
NTU	-	-	-	-	-	-	-	-
EC	-	-	-	-	0.832	0.839	643	624

930



931 Table A6. Model evaluation of R_{eco} and GPP models using all data pooled and modelling all
 932 blocks and harvest treatments all together “field model”

R_{eco} model	R^2	0.78
	NRMSE	46.6
	NSE	0.78
	AIC c	14223.49
GPP model	R^2	0.88
	NRMSE	34.2
	NSE	0.88

933 The four indexes of model evaluation are: R^2 , normalized root mean square of error
 934 (NRMSE), Nash-Sutcliffe efficiency (NSE), and corrected Akaike Information Criteria.

935



936 Table A7. Carbon budget results obtained by using all data pooled and modelling all blocks
937 and harvest treatments all together to obtain field models of R_{eco} and GPP.

Block	Treatment	Reco	GPP	NEE	Yield	NECB
		t CO ₂ -C ha ⁻¹ yr ⁻¹	t CO ₂ -C ha ⁻¹ yr ⁻¹	t CO ₂ -C ha ⁻¹ yr ⁻¹	t C ha ⁻¹ yr ⁻¹	t C ha ⁻¹ yr ⁻¹
A	0-cut	21.1	-16.9	4.2	NA	4.2
B		18.8	-15.6	3.2	NA	3.2
C		21.6	-16.6	5.0	NA	5.0
D		23.0	-19.2	3.8	NA	3.8
Mean ± SE		21.1 ± 1.6	-17.1 ± 1.3	4.1 ± 0.7	NA	4.1 ± 0.7
A	2-cut	21.9	-17.5	4.4	1.9	6.3
B		22.4	-19.3	3.1	4.5	7.7
C		23.7	-18.4	5.3	4.6	10.0
D		22.1	-16.6	5.5	5.0	10.6
Mean ± SE		22.6 ± 0.7	-17.9 ± 1	4.6 ± 1	4 ± 0.7	8.6 ± 1.7
A	5-cut	23.9	-19.4	4.4	3.5	7.9
B		23.7	-20.8	2.9	3.9	6.7
C		25.7	-20.7	5.0	3.5	8.5
D		23.8	-20.3	3.5	4.5	8.0
Mean ± SE		24.3 ± 0.8	-20.3 ± 0.6	3.9 ± 0.8	3.8 ± 0.2	7.8 ± 0.7

938

939 R_{eco} is ecosystem respiration, GPP is gross primary productivity, NEE is net ecosystem
940 exchange, and NECB is net ecosystem carbon balance (NEE + yield).